https://doi.org/10.5194/egusphere-2026-6376
Preprint. Discussion started: 23 November 2026
© Author(s) 2026. CC BY 4.0 License.

Decoupling of fire activity from hydroclimate during the Late Holocene in central Chile

Carolina Godoy-Aguirre[1], Matías Frugone-Álvarez[2], Magdalena Fuentealba[3], Josué M Polanco-Martínez[4], Antonio Maldonado[5,6], Mauricio Gallegos[7], Roberto Campbell[8], José Iriarte[9], Blas Valero-Garcés[10], Claudio Latorre [7,11]

[1]Departamento de Antropología, Universidad Alberto Hurtado, Santiago, Chile.
[2] Instituto de Alta Investigación, Universidad de Tarapacá, Arica, Chile.
[3] Instituto de Geografía, Pontificia Universidad Católica de Chile, Santiago, Chile.
[4] Departamento de Economía, Área de métodos cuantitativos, Universidad de Santander, Santander, España.
[5] Centro de Estudios Avanzados en Zonas Áridas (CEAZA), La Serena, Chile.
[6]Vicerrectoría de Investigación y Postgrado, Universidad de La Serena, La Serena, Chile
[7] Centro UC Desierto de Atacama & Facultad de Ciencias Biológicas, Pontificia Universidad Católica de Chile, Santiago, Chile.
[8] Escuela de Antropología, Pontificia Universidad Católica de Chile, Santiago, Chile.
[9] Department of Archaeology, College of Humanities, University of Exeter, Exeter, UK.
[10] Pyrenean Institute of Ecology (CSIC), Zaragoza, España.
[11] Institute of Ecology and Biodiversity (IEB), Santiago, Chile.

Correspondence to: Claudio Latorre (clatorreh@uc.cl)

Abstract. The long-term role human societies play in shaping fire regimes, especially in relation to climate change, remains unresolved. We present a 3,000-year multiproxy high-resolution reconstruction from Lake Vichuquén (34.8°S), integrating macroscopic charcoal, pollen, phytoliths, biogeochemical proxies, and archaeological data. Prior to ca. 1,200 cal yr BP, decadal-to-interdecadal variability of charcoal accumulation is consistent with hydroclimatic variability linked to the El Niño–Southern Oscillation and Pacific Decadal Oscillation. Increasing archaeological activity, more open vegetation, and the establishment of horticultural practices, point to climate variability and human land use as contributors to the fire regime. After ca. 1,200 cal yr BP, charcoal accumulation declined sharply despite persistent horticulture and regional occupation along with hydroclimate variability. Continued climate variability in catchment proxies and subsequent recovery of charcoal accumulation indicate that depositional change alone cannot explain the decline. The charcoal record thus became decoupled from its earlier hydroclimatic relationship even as land use intensified during the Inka and Colonial periods. A further reorganization occurred in the 20th century, when exotic tree plantations, increasing woody vegetation, and prolonged drought coincided with a marked rise in charcoal accumulation. In contrast, the January 2017 megafire produced the largest charcoal peak in the entire 3,000-year sequence. These results demonstrate that long-term fire regimes in central Chile were shaped by changing, non-linear interactions among hydroclimate, vegetation, and human land use.

https://doi.org/10.5194/egusphere-2026-6376
Preprint. Discussion started: 23 November 2026
© Author(s) 2026. CC BY 4.0 License.

1 Introduction

Fire regimes are processes that shape landscapes and ecosystem functioning and are closely linked to climate change and fuel availability (e.g. biomass), including their connectivity and flammability characteristics (Keeley, 2012; Whitlock et al., 2010). Human activities, including altered ignition rates, timing of burning, and fuel management through changes in vegetation cover, can modify intensity and frequency of fires (Bowman et al., 2011; Calo, 2014; Whitlock et al., 2010). Other crucial factors are population density, changes in land use, and social, economic and technological developments (Roos et al., 2014). Reconstructing the history of interactions between people, climate change, and fire is essential to understanding long-term fire regimes and ecosystem dynamics (Armstrong et al., 2017; Whitlock et al., 2010).

Across Mediterranean-type ecosystems, human activities are an important source of fire ignition, but this imbalance between anthropogenic and natural ignitions is particularly pronounced in central Chile (Abarzúa et al., 2016; González et al., 2011; Keeley, 2012). Natural lightning ignitions are exceptionally rare in the region because the Andes largely prevent moist subtropical storms with convective lightning from reaching central Chile from the east (Keeley, 2012). Recent wildfire activity has been clearly linked to humans and large-scale forest plantations, amplified by extreme weather and ENSO (El Niño-Southern Oscillation) variability, often with catastrophic consequences (Carrasco-Escaff et al., 2024; Cordero et al., 2024; Gomez-González et al., 2019; Urrutia-Jalabert et al., 2018). Existing microcharcoal studies from lacustrine records show that fire regimes have exhibited ENSO-like variability over the past millennia (Martel-Cea et al., 2016; Villa-Martínez, 2002; Villa-Martínez et al., 2003; 2004). This could be explained by large amounts of biomass accumulating in watersheds during El Niño-type phases, which are then converted into dry fuels with good connectivity during ensuing cold and dry La Niña-type phases (González et al., 2011). Pollen and microcharcoal records further show that increased charcoal accumulation was also accompanied by pollen from plants with high moisture requirements (Villa-Martinez, 2002), suggesting that fires increased during wet phases.

The potential human influence on fire regime alterations during pre-Hispanic times remains a topic of ongoing debate in central Chile. Some researchers suggest that practices such as land clearing for cultivation, habitation, and hunting may have contributed to changes in fire regimes and modifications of the vegetation landscape (Aravena et al., 2003; Armesto et al., 2009; 2010; Heusser, 1983; Rozas et al., 2018; Simonetti and Cornejo, 1990; Villa-Martínez et al., 2003). Human groups from the Early Ceramic Period (300 BCE - 1200 CE) likely practiced small-scale slash-and-burn agriculture during the early stages of agricultural activity in the region (Sanhueza et al., 2007), with subsequent intensification of pressures on vegetation associated with periods of increased prehistoric agricultural production (Planella et al., 2014). In contrast, most studies suggest that human activity played a predominant role in shaping fire regimes only after European colonization (1541 AD), attributing most earlier large-scale fires to climatic variability which minimizes the influence of pre-Hispanic human activity into possible landscape management practices (Villa-Martínez, 2002; Villa-Martínez et al., 2003; Martel-Cea et al., 2016).

Amidst the escalating global changes affecting Mediterranean climates, characterized by a dry season coinciding with the warmest period of the year, long-term ecosystem reconstructions are particularly important for understanding fire dynamics and their responses to environmental change. This endeavor involves not only analyzing environmental dynamics but should necessarily address and recover the histories of human communities that inhabited and shaped these landscapes (Balée, 2006; Crumley, 2021). Indeed, such narratives are now essential for understanding the environmental and cultural transformations within these territories.

This study investigates how cultural and climatic changes influenced the fire regime in south-central coastal Chile. We focussed on two key time periods: 1) the transition from hunter-gatherer to agricultural societies in the Late Holocene, and 2) the last 100 years when major landscape transformations occurred due to increased anthropogenic activities. To achieve this, we develop a high-resolution macrocharcoal record spanning the past 3,000 years from Lake Vichuquén. Additionally, we analyze phytoliths and pollen to track vegetation changes and use stable isotope bulk sediment analysis to examine lake ecosystem dynamics. By comparing our findings with other regional paleoenvironmental and archaeological records, we examine changes in past and present fire dynamics alongside cultural and climatic transitions in this Mediterranean-type ecosystem.

https://doi.org/10.5194/egusphere-2026-6376
Preprint. Discussion started: 23 November 2026
© Author(s) 2026. CC BY 4.0 License.

2 Study area

2.1 Vichuquén, a coastal lake in the Maule region

Lake Vichuquén (34°49′S, 72°04′W; 4 masl) is located in the northern part of the Maule region, and it is placed between 3 to 6 km from the coastline, with a maximum water depth of ~ 33 m and a lake surface of 40 km2 (Fig. 1). The lake is fed by two main rivers, the Vichuquén and Huiñe Rivers, and drains into the Pacific Ocean through the Llico estuary. The current vegetation of the area corresponds mostly to grasslands, non-native shrubs (*Rubus ulmifolius*) or cultivated areas with exotic tree plantations of *Eucalyptus globulus* and *Pinus radiata* (Frugone-Álvarez et al., 2018; Fuentealba et al., 2021; Ramírez et al., 2014). In addition, much of the lakeshore and surrounding area is mostly developed, with large houses and tourist centres, although some traces of native mediterranean vegetation remain in areas of coastal ravines, including sclerophyllous scrub or matorral chileno and sclerophyllous forest of *Lithrea caustica* and *Azara integrifolia* (Armesto et al., 2007; Torres-Ramírez et al., 2017).

Previous records have reconstructed the environmental evolution of the lake spanning the last 7,000 cal yr BP with relatively high-resolution that varies between <2 to 4.7 yr cm^{-1} (Frugone-Álvarez et al., 2017) and is thus an ideal site for detailed reconstruction of past fire dynamics. Prior to 2,200 cal yr BP, the basin was open to the Pacific and characterized by marine, open, relatively shallow lagoon environments, whereas afterwards, the connections with the Ocean became restricted and lacustrine environments have dominated since 1,200–1,000 cal yr BP (Frugone-Álvarez et al., 2017). The region has a Mediterranean climate characterized by rainfall concentrated almost exclusively in the winter months (June to August) and hot and dry summer months (December to February) (Armesto et al., 2007). This marked seasonality responds to the northward movement of the South Pacific Anticyclone (SPA) during winter months, allowing the entry of rainy fronts associated with the Southern Westerly Wind Belt (SWW) (Garreaud, 2009). On the contrary, during the summer months SPA is reinforced blocking the frontal systems (Garreaud, 2009; Montenegro et al., 2003). Climate variability at interannual and interdecadal scale is influenced by ENSO and the Pacific Decadal Oscillation, (PDO) and Southern Annular Mode (SAM) (Grez et al., 2020; Garreaud et al., 2020).

During the last 3,000 years, central Chile underwent a transition from predominantly hunter-gatherer societies to economies in which horticulture and, later, agriculture and pastoralism became increasingly important. This process involved changes in settlement patterns and social organization and culminated in the expansion of the Inka estate during the Late Period (Cornejo et al., 2016; Falabella et al., 2016; Planella et al., 2014; Uribe and Sánchez, 2016). At the local scale, the Vichuquén–Laguna Torca system contains evidence of human occupation dating back to at least the Late Holocene, including the burial known as Mujer de Totorilla, the Paula archaeological site, shell middens near the mouth of Estero Llico, and other sites recorded around the lake and adjacent coastal environments (CONAF, 1990; Cornejo, 1988; Stehberg and Quevedo, 1988). Although this area has received considerably less archaeological attention than other parts of central Chile, surveys reported in the management plan of Reserva Nacional Laguna Torca documented sites containing lithic and ceramic materials both within and around the reserve (CONAF, 1990). Archaeological and ethnohistorical evidence further

https://doi.org/10.5194/egusphere-2026-6376
Preprint. Discussion started: 23 November 2026
© Author(s) 2026. CC BY 4.0 License.

indicates an Inka presence in the area during the Late Period, followed by the progressive incorporation of the region into the colonial economy through agriculture, livestock husbandry, timber extraction, salt production, and vineyard labor (Frugone-Álvarez et al., 2018; Odone, 1998). Currently, more than 60% of the basin is covered by pine plantations, largely as a result of state policies that subsidized forestry expansion in Chile following the Decree Law 701 (1974) (Fuentealba et al., 2021).

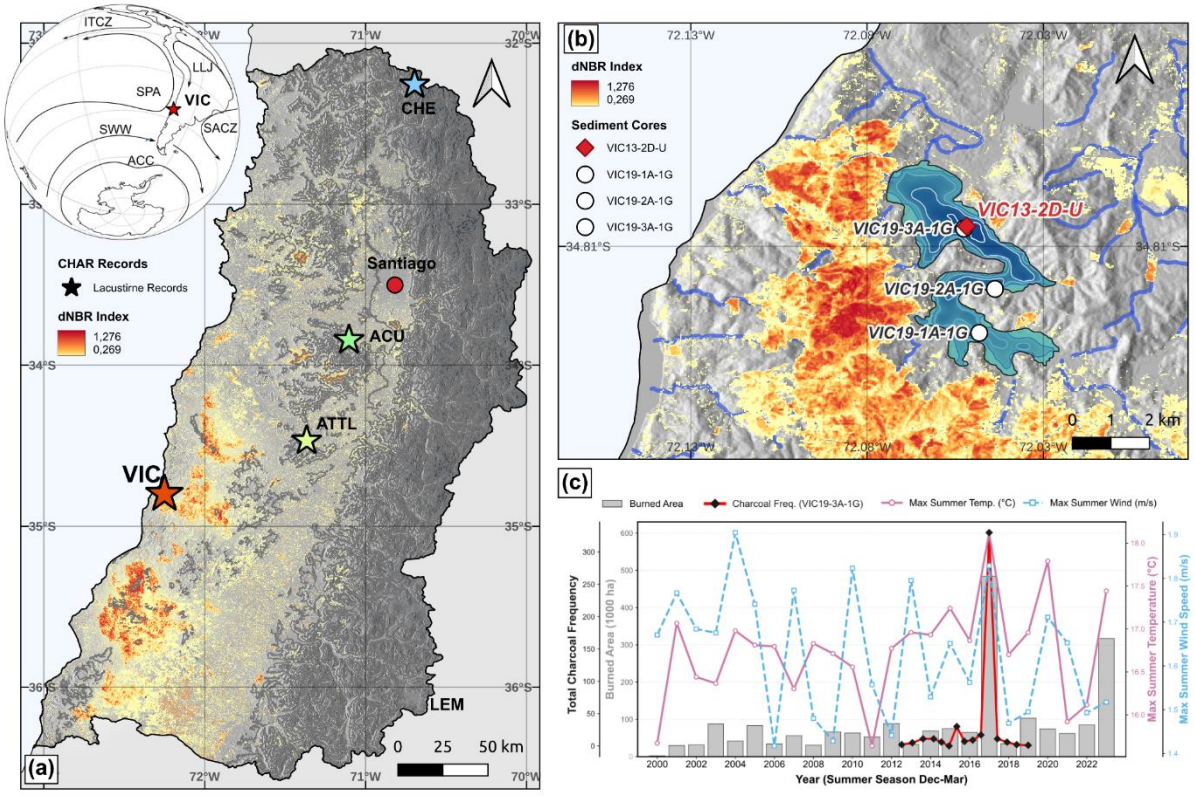

Fig. 1. Regional context of the 2017 megafire, lacustrine sedimentary records, and fire-climate dynamics in central Chile.

(a) Spatial distribution of the 2017 fire severity (dNBR index) derived from Landsat 8 imagery. Stars indicate the location of the lacustrine Charcoal Accumulation Rate (CHAR) records discussed in the text. The inset displays the large-scale atmospheric circulation patterns forcing the regional climate, including the Intertropical Convergence Zone (ITCZ), the South Pacific Anticyclone (SPA), the Southern Westerly Winds (SWW), and the Antarctic Circumpolar Current (ACC). (b) Lake Vichuquén catchment showing local fire severity and the locations of the retrieved sediment cores (VIC13-2D-U, VIC19-1A-1G, VIC19-2A-1G, and VIC19-3A-1G). (c) Temporal evolution (2000–2022) of the regional burned area, maximum summer temperature, maximum summer wind speed, and the reconstructed total charcoal frequency derived from the VIC19-3A-1G sediment core.

3. Methods

3.1 Core sampling and chronology

https://doi.org/10.5194/egusphere-2026-6376
Preprint. Discussion started: 23 November 2026
© Author(s) 2026. CC BY 4.0 License.

We sampled the upper 7 m of the composite sedimentary sequence VIC13, which comprises the long cores VIC13-2D and VIC13-2A, and the short core VIC13-2B-1G (Fig. A1). Lithostratigraphic units and sedimentary facies definitions for the studied sequence follow Frugone-Álvarez et al. (2017). Furthermore, in August 2019, a modified UWITEC gravity core was utilized to obtain three short cores at three distinct depths (VIC19-3A-1G; 30 m, VIC19-2A-1G; 20 m, VIC19-1A-1G; 10 m). The VIC19-3A-1G short core was collected at the same location as the VIC13 sequence (see Fig. 1). These sediment cores were correlated with sedimentological, TOC, TIC and TS data, which were subsequently used for charcoal analysis. The short cores were used to identify chronostratigraphic marker of the 2017 "mega-fire" event that affected central Chile (Pliscoff et al., 2020), particularly important for the Llico-Torca-Vichuquén wetland complex, where around 258 ha were affected by the fire (CONAF, 2017).

A revised age-depth model for the composite sequence was developed by integrating the 14C dates published by Frugone-Álvarez et al. (2017) with newly 210Pb data. We add the most recent megafire event of January 2017 as a chronostratigraphic marker in the sequence and a reservoir effect of 180 ± 25 14C years, as determined by dissolved inorganic carbon (DIC) dating of water. We integrated the previously published sedimentary facies and units from Lake Vichuquén into the new chronological framework (Fig. A1). The age-depth model was constructed using the R rplum package for Bayesian 210Pb/14C age-depth modeling (Aquino-López et al., 2018; Blaauw and Christen, 2011). Radiocarbon ages were calibrated using the Southern Hemisphere calibration curve (Hogg et al., 2020).

3.2 Macro charcoal analysis

We sampled 2 cm^3 of wet sediment per centimeter from a 7-meter VIC13 composite sequence and three short cores from 2019 (first 15 cm) (Figs. A1 and B1). The VIC19-3A-1G short core was selected to represent the 2017 megafire event (peak at 5 cm), which was correlated with the VIC13 sequence and analyzed in conjunction with other proxies. A total of 737 samples were immersed in 3% hydrogen peroxide for a 24-hour period. Then, the samples were sieved through 106 and 212 µm mesh screens and counted them on a stereomicroscope (Moreno et al., 2012; Whitlock and Anderson, 2003; Whitlock and Larsen, 2002). Grass and woody charcoal were differentiated based on anatomical structure (Whitlock et al., 2006). Charcoal accumulation rate (CHAR; particles cm^{-2} $year^{-1}$) was calculated using CharAnalysis software (Higuera et al. 2009) by linearly interpolating charcoal measurements to a median resolution of 4 years. Low frequency CHAR (Cback) was estimated using a LOWESS regression with a 250-year window (global signal-to-noise index = 4.3). High frequency CHAR (C_{peak}) was calculated by subtracting C_{back} from the interpolated signal. Individual fire events (Peaks Final) were identified based on values surpassing a locally defined threshold determined by the 99th percentile of a Gaussian distribution of C_{noise} component. Fire episode magnitude (Peak magnitude, cm^{-2} $peak^{-1}$), fire episode frequency (fire yr^{-1}), and fire return intervals (smFRIs) were calculated using a 250-year smoothing window. Additionally, a grass-to-total charcoal ratio was estimated based on anatomical structure results in the time series (Whitlock et al., 2010).

https://doi.org/10.5194/egusphere-2026-6376
Preprint. Discussion started: 23 November 2026
© Author(s) 2026. CC BY 4.0 License.

3.3 Pollen analysis

Fifty-four pollen samples were obtained from long core VIC13 and processed following the methods of Faegri and Iversen (1989) to extract pollen grains. *Lycopodium* tablets were added to calculate pollen concentrations (grains cm^{-3}) and accumulation rates (grains cm^{-2} yr^{-1}; Stockmarr, 1971). Pollen grains were mounted on glass slides and identified and quantified using an Axiostar Carl Zeiss microscope at 400× and 1000× magnification, a published pollen atlas (Heusser, 1971), and the reference pollen collection of the Paleoecology Laboratory at CEAZA. Pollen counts targeted 300 terrestrial pollen grains per sample, excluding paludal taxa, although this total was not reached in some samples, particularly those from the last ca. 100 years, due to low pollen concentrations.

The arboreal/non-arboreal pollen index (AP/NAP index) was calculated using Eq. (1) (Maher, 1963, 1972):

$$\text{AP/NAP index} = \frac{a}{a+b} \times 100 \quad (1)$$

where 'a' represents the abundance of Arboreal pollen and 'b' represents the abundance of No-Arboreal pollen (Maher, 1963, 1972). In this way, values near 100 in the pollen index suggest a high proportion of arboreal pollen, which generally reflects more humid conditions, whereas values near 0 suggest a predominance of non-arboreal pollen, indicating drier conditions.

3.4 Phytolith analysis

We extracted phytoliths from approximately 2 g of sediment, spaced every 30 cm of the composite sedimentary sequence VIC13 to reconstruct general trends of local vegetation change (Aleman et al., 2014; Rasbold et al., 2020). Following standard procedures (Piperno, 2006), we used 36% HCl and 70% HNO3 to remove carbonates and organic matter. Phytoliths were separated by heavy liquid flotation using ZnBr2 with a density of 2.3 g/cm3 (Dickau et al., 2013). We counted 200 phytoliths per sample (Pearsall, 2016; Piperno, 2006) and calculated the percentage of each phytolith type as a relative frequency. Main phytolith morphotypes were identified using the reference collection at the Archaeobotany Laboratory, University of Exeter, and ICPN group criteria when applicable (ICPT, 2019). Possible maize leaf phytoliths were studied using discriminant function measures in cross-shaped phytoliths (cross variants 1 and 5/6) (Piperno, 2006).

3.5 Biogeochemical analysis

Stable isotope compositions ($\delta^{13}C$ and $\delta^{15}N$), total organic carbon (Corg), and total nitrogen (TN) of bulk organic matter were analyzed in sediment samples collected at 5 cm intervals from composite sequence VIC13. Approximately 20 mg of each sample was weighed and analyzed using a Delta V Advantage IRMS coupled to a Thermo Flash 2000 at the Laboratory of Biogeochemistry and Applied Stable Isotopes at PUC (LABASI-PUC). For $\delta^{13}C$ and Corg analyses, carbonates were

https://doi.org/10.5194/egusphere-2026-6376
Preprint. Discussion started: 23 November 2026
© Author(s) 2026. CC BY 4.0 License.

removed using 200 µL of deionized water and 50 µL of 3:1 v/v HCl, and the samples were subsequently dried at 50 °C for 4 h (Harris et al., 2001). In addition, the molar C/N ratio was calculated for each sample using Eq. (2) (Meyers, 2003):

$$(C/N)_{\text{molar}} = \frac{C_{\text{org}}/12}{\text{TN}/14} \quad (2)$$

Data for the last 400 years were obtained from Fuentealba et al. (2021).

3.6 Statistical analysis

Pollen, phytolith and CONISS diagrams and index were generated using the R packages tidyverse v0.2.0.0 (Wickham et al. 2019), tidypaleo v0.1.1 (Simpson et al. 2023), ggplot2 v3.3.5 (Wickham 2016), vegan v2.6-10 (Oknasen 2016), and rioja v0.9-26 (Juggins, 2023). Regime shifts across the proxy time series were identified using change-point analyses. Transitions in the arboreal phytolith sequence were assessed using the "changepoint" package in R (Bai and Perron, 2003; Killick and Eckley, 2014) to identify shifts in mean and variance under the PELT algorithm. Concurrently, the charcoal (CHAR) and geochemical time series were evaluated in Python using the "ruptures" package via a non-parametric PELT implementation with a Radial Basis Function (RBF) kernel. Analyses on the latter were conducted on standardized (z-scores) interpolated series (4-yr resolution), constrained by a minimum segment length of 40 yr (10 steps) and a penalty value of 5 to avoid detecting spurious short-term fluctuations

Published paleoclimate series were compiled for time-series statistical analysis, comprising XRF elemental ratios (Rb/Sr, Br/Ti, K/Ti) from Lake Vichuquén (central Chile; Frugone-Álvarez et al., 2017), lithic concentration profiles from marine core SO147-106KL (offshore Peru; Rein et al., 2005), and XRF records from Laguna Pallcacocha (Ecuadorian Andes; Mark et al., 2022). For the Vichuquén record, the K/Ti ratio reflects detrital terrigenous supply and physical weathering. In contrast, the Rb/Sr ratio is employed as a proxy for effective basin water balance, where elevated Rb reflects fluvial silicate discharge under positive moisture regimes, whereas Sr enrichment records evaporative concentration, authigenic carbonate precipitation, and/or marine incursions during negative water-balance intervals (Chen et al., 1999; Jin et al., 2001, Kalugin et al., 2005; Darin et al., 2015). Br/Ti ratio is associated with organic productivity (see Frugone-Álvarez et al. 2017; Kalugin et al., 2005). To assess the influence of multi-decadal to centennial climate variability on fire regimes in central Chile, we performed spectral analysis on unevenly spaced series using REDFIT (Schulz and Mudelsee, 2002) and resolved non-stationary periodicity using the Weighted Wavelet Z-transform (WWZ; Foster, 1996) (Supplementary Code; see Zenodo research compendium).

REDFIT is a spectral analysis method specifically designed for unevenly spaced paleoclimate time series. It estimates the power spectrum while explicitly accounting for the red-noise background, modeled as a first-order autoregressive (AR1) process. By comparing observed spectral peaks against this red-noise background, REDFIT identifies statistically significant spectral peaks (possible periodicities) while controlling for the autocorrelation inherent to paleoclimate records, making it particularly suitable for proxy records such as sediment cores, tree rings, and ice cores. Before applying REDFIT, each palaeoclimate record was linearly detrened to satisfy the assumption of stationarity. Spectral peak significance was tested at

https://doi.org/10.5194/egusphere-2026-6376
Preprint. Discussion started: 23 November 2026
© Author(s) 2026. CC BY 4.0 License.

the 90 %, 95 % and 99 % confidence levels. REDFIT spectra were generated with the original Fortran 90 implementation (v3.8) (Schulz & Mudelsee, 2002). Wavelet spectral analyses were performed on the unevenly spaced paleoclimate time series using the Pyleoclim Python package (v 1.0.0; Khider et al., 2022). Pyleoclim implements the Weighted Wavelet Z-transform (WWZ; Foster, 1996), which estimates localized time–frequency power by projecting the time series onto a set of sinusoidal basis functions weighted according to temporal proximity. To accommodate irregular sampling and heteroscedasticity inherent in paleoclimate proxies, the WWZ in Pyleoclim incorporates adaptive weighting and bias-correction refinements following Kirchner and Neal (2013), enabling unbiased estimation of spectral power directly at the original chronological resolution without interpolation. The resulting WWZ power spectrum provides a robust measure of the amplitude and significance of oscillatory components over time, accounting for both local variance and red-noise characteristics of climate signals. Individual (univariate analysis) WWZ power spectra were first computed for each series to identify significant periodicities. Time–frequency covariability (bi-variate analysis) between datasets was then assessed using the Cross-Wavelet Transform (XWT) and Wavelet Coherence (WTC). Specifically examining relationships between charcoal accumulation rates, XRF element ratios, and ENSO proxies (Appendix A, sections A2 and A3, for details).

To explore the temporal distribution of available archaeological dates at a subregional scale, a Summed Probability Distribution (SPD) was constructed using 90 dates from 41 archaeological sites in the Maule Region. The dataset comprises 82 thermoluminescence (TL) dates and eight radiocarbon dates from published archaeological records spanning 34.83° and 35.98°S (Godoy-Aguirre et al., 2024). TL ages were converted to years BP using 1950 CE as the reference year and treated as normal distributions, whereas radiocarbon dates were calibrated using the SHCal20 curve (Hogg et al., 2020). To reduce overrepresentation of intensively dated sites, dates were binned by site using a 50-year threshold before summation (Crema and Bevan, 2021). The SPD was calculated using the rcarbon package in R (Crema and Bevan, 2021), without normalization, and smoothed using a 150-year moving average (see Zenodo research compendium). The resulting SPD is used as a general index of temporal variation in the available archaeological dates.

4 Results

4.1 Carbon and Nitrogen lake signatures of watershed dynamic

The composite sedimentary sequence spans ca. 3,000 cal yr BP, with an average sedimentation rate of ca. 5 yr/cm (Fig. A2). The rate of accumulation is relatively constant but with a noticeable decrease over the last 100 years. (Fig. A2). The C_{org} content and $\delta^{13}C$ are mostly coupled throughout the sequence (Figs. 2a-b). An upward trend (more positive $\delta^{13}C$ and higher C_{org} content) during deposition of brackish marine Unit 3 and the lower part of brackish-fresh Subunit 2B (-19.8 ± 2.6 ‰ $\delta^{13}C$ and 634 ± 164.6 µg/g C_{org}) from 3,000 years to about 1,750 cal yr BP. Alongside this trend, variability increased from about 2,250 cal yr BP. Between 1,750 and 1,250 cal yr BP (upper part of subunit 2B), $\delta^{13}C$ values are slightly more negative and C_{org} remains in a similar range to the previous period (-20.9 ± 0.9 ‰ $\delta^{13}C$ and 692 ± 120 µg/g C_{org}). Towards the end of Subunit 2B, there is evidence of a sharp decline in organic carbon accumulation. Values between ca. 1,250 and 500 cal yr BP

https://doi.org/10.5194/egusphere-2026-6376
Preprint. Discussion started: 23 November 2026
© Author(s) 2026. CC BY 4.0 License.

are the lowest recorded throughout the analyzed sequence (-25.6 ± 1.3 ‰ $\delta^{13}C$ and 311 ± 107 µg/g Corg, 1,250–470 cal yr BP) (Fig. B3). The most recent record (Fuentealba et al., 2021) documents a slight increase in Corg content during historical times and especially during the last decades, and a change in the Corg - $\delta^{13}C$ relationship, as $\delta^{13}C$ values during the last decades were again among the lowest in the sequence.

The C/N_{molar} ratio (Fig. 2c) values range from 5 to 18, with most values around 10, indicating a dominant algal origin of the organic matter (Meyers and Teranes, 2002). These values are increasing from the base of the record, until they reach relatively higher C/N_{molar} ratios between 2,300 and 1,700 cal yr BP; from the latter date a downward trend in C/N_{molar} ratio begins, reaching the lowest values around 1,000 cal BP. Between ca. 1,000 and 500 cal yr BP, values remain the lowest of the sequence, followed by an increase from ~500 cal yr BP onward to the present. Additionally, $\delta^{13}C$ values closely parallel the trend observed in the C/N_{molar} ratio throughout the studied record (3,000–500 cal yr BP) (Fig. B2b).

Conversely, $\delta^{15}N$ values are more variable over time (Fig. 2d), although three main periods with slightly different trends are observed. First, an increasing trend during brackish, marine Unit 3 between 3,000 and 2,200 cal yr BP (5.13 ± 0.5 ‰). Subsequently, there is a slight downward trend beginning with the onset of facies 2B (c. 2,200 cal yr BP) and up to 1,550 cal yr BP (4.63 ± 0.4 ‰ $\delta^{15}N$), although with some marked variability after 2,250 cal yr BP. Later, during the transition from Unit 2 to 1 the range is larger ($\delta^{15}N$ = 5.31 ± 0.7 ‰) but with a generally positive trends. The short cores show an increase in TN and a sharp decrease in $\delta^{15}N$, reaching the lowest values in the entire record (about 3 ‰) during the last decades (Fuentealba et al., 2021).

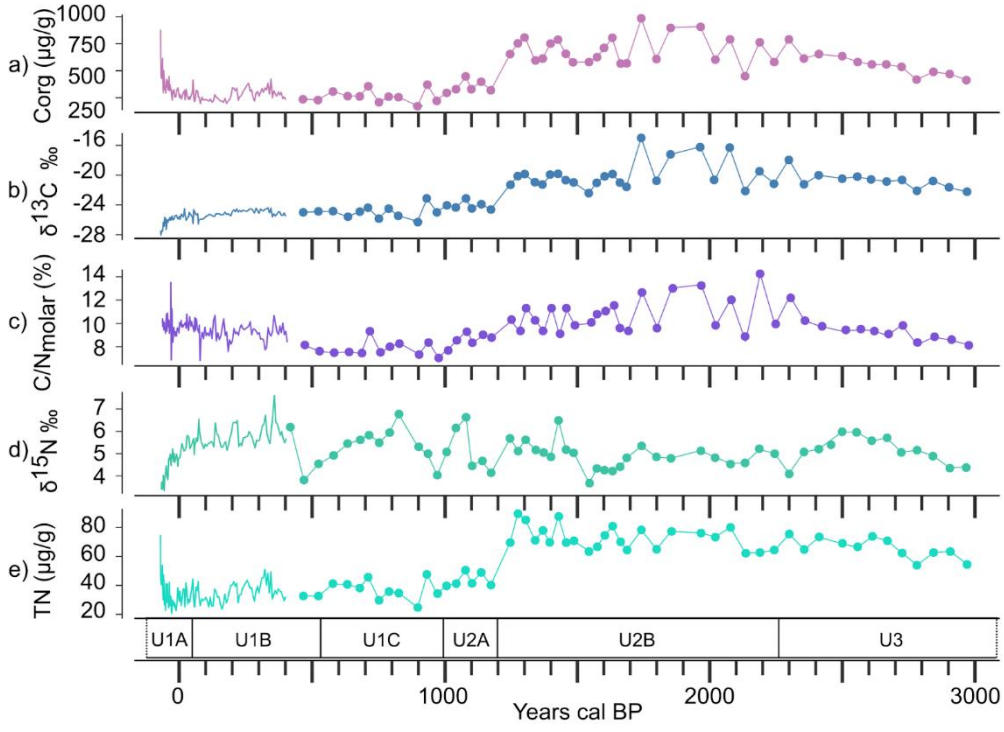

https://doi.org/10.5194/egusphere-2026-6376
Preprint. Discussion started: 23 November 2026
© Author(s) 2026. CC BY 4.0 License.

Fig. 2. Geochemical signatures in the composite sequence VIC13.

(a) Total Organic Carbon µg/g (Corg). b) δ13C ‰ values. c) C/Nmolar ratio. d) δ15N ‰ values. e) Total Nitrogen µg/g (TN). The solid line in figures a to e corresponds to data from Fuentealba et al., 2021, the dotted line corresponds to this study. Basal sedimentological units follow Frugone-Álvarez et al. (2017): Unit 1A comprises dark laminated, diatom-poor muds dominated by quartz and chlorite; Unit 1B consists of laminated muds characterized by high magnetic susceptibility, moderate C/N ratios, and a complete absence of calcite; Unit 1C marks the onset of a stable lacustrine regime with dark muds, the conspicuous appearance of detrital quartz, and sharp declines in Corg, TN, and BioSi; Unit 2A records a brackish-to-freshwater transition accompanied by a gradual decrease in Corg and the progressive loss of evaporitic calcite/gypsum in banded-to-laminated muds; Unit 2B encompasses very finely laminated muds exhibiting sequence maxima in Corg , TS, BioSi, and high C/N ratios, associated with authigenic pyrite peaks under bottom-water anoxia; and Unit 3 is dominated by laminated muds with clastic intercalations, rich in calcite and gypsum within a brackish coastal lagoon.

4.2 Macro-charcoal analysis

The Vichuquén record shows an upward trend in charcoal accumulation rate (CHAR) and Cpeak from about 3,000 to 1,200 cal yr BP (Units 3 and 2), followed by a sharp decrease after 1,200 cal yr BP (transition to Unit 1) (Fig. 3a). CHAR and Cpeak show an increasing trend between about 3,000 and 1,200 cal yr BP. This upward trend is interrupted by a medium-magnitude event around 2,800 cal yr BP and two high-magnitude events around 2,680 and 2,400 cal yr BP (Fig. 3a). From 3,000 to 2,300 cal yr BP, the ratio of grass to total charcoal shows an average of 0.24. Subsequently, a slight decrease in CHAR and Cpeak is observed between 2,300 and 2,100 cal yr BP. The magnitude of the events in this interval is moderate to low, and the grass to total charcoal ratio has a mean of 0.21. A new period of increase in CHAR and Cpeak is detected between 2,100 and 1,700 cal yr BP. This interval represents a relative alternation of low to medium-high magnitude events. It is accompanied by a grass to total charcoal ratio of 0.27 on average (Fig. 3a and c). Between 1,700 and 1,580 cal yr BP there was a slight decrease in CHAR and Cpeak. In addition, the events in this period are of low magnitude, with a mean grass to total charcoal ratio of 0.17. Between ca. 1,580 and 1,380 cal yr BP there is a generalized increase in CHAR and Cpeak, with events of medium-low magnitude and a mean of 0.22 in the grass to total charcoal ratio. Subsequently, between ca. 1,380 and 1,200 cal yr BP, a trend toward a decrease in CHAR began, followed by events of medium to low magnitude and a mean percentage of grass to total charcoal of 19.16%. This corresponds to transitional unit 2A (1,200-1,000 cal yr BP). Later, CHAR and Cpeak decreased significantly, with temporary increases around 970 and 680 cal yr BP, where medium-high and low magnitude events were recorded, respectively. CHAR and Cpeak show a recovery from about the first half of the 20th century (1930 CE), culminating in peaks at the end of the sequence in both CHAR and magnitude.

The mean grass to total charcoal ratio for the period after 1,200 cal yr BP is 0.23 while its value from the beginning of the 20th century to the present is 0.31. The grass to total charcoal ratio shows a global mean of 0.23 for the entire sequence, and a pattern of high variability in this ratio is observed throughout the record. A total of 52 "fire events" (Peak Final) were recognized, 48 of which occurred in prehispanic times, 9 of which were concentrated before 2,500 cal yr BP, 33 events between 2,500 and 900 cal yr BP, and 6 between 800 and 650 cal yr BP, and finally four fire events occurred in historic

https://doi.org/10.5194/egusphere-2026-6376
Preprint. Discussion started: 23 November 2026
© Author(s) 2026. CC BY 4.0 License.

times, including the January 2017 megafire event (Fig. 3). The peak frequency tends to decrease between 3,000 and 2,770 cal yr BP, and then we observe a sustained increase until about 2,640 cal yr BP (Fig. 3d).

Later, the frequency has a slight decrease until 2,250 cal yr BP to resume a period of increase between 2,250 and 1,800 cal yr BP. From 1,800 to 1,600 cal yr BP, the frequency shows a decreasing trend, which steadily returns between 1,600 and 1,300 cal yr BP. The frequency decreases again between about 1,300 and 1,110 cal yr BP to recover from this last point to about 740 cal yr BP. From 740 to 500 cal yr BP, the frequency of fires decreased steadily to reach minimum values between 500 and 300 cal yr BP. After this last date, the frequency of fires begins a sustained increase to the present.

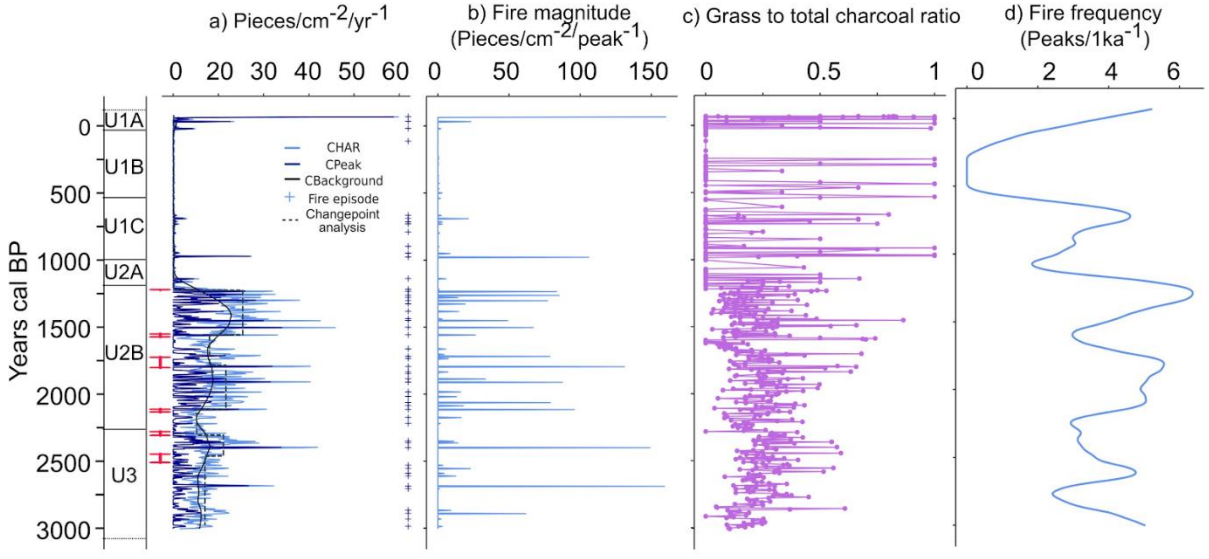

Fig. 3. CharAnalysis for the compiled macro charcoal record of Lake Vichuquén spanning the last 3000 cal yr BP.

(a) Charcoal accumulation rate (CHAR). Grey dotted lines indicate the changepoints identified by the changepoint analysis, and red lines indicate their associated 95% confidence intervals.

4.3 Vegetation dynamics inferred from phytolith analyses

The Vichuquén phytolith assemblage is composed of the Poaceae, Cyperaceae, Asteraceae, and Arecaceae families, with the subfamilies and genera Bambusoideae, Panicoideae, cf. *Stipa*, *Aristida*, Chloridoideae, and Pooideae morphotypes (Fig. 4). Phytoliths of woody dicotyledonous plants were grouped into an "arboreal" category, representing in a coarse form species such as trees and scrubland. The plants identified at the species level correspond to cf. *Zea mays*, from which wavy upper rondels and phytoliths indicating the presence of leaves were recovered (Table B1, Appendix B) and the only palm native to the region (*Jubaea chilensis*) in the case of Arecaceae phytoliths. Furthermore, the Bambusoideae category corresponds to *Chusquea* spp. (Muñoz and González, 2009). The assemblage changes show an initial stable period (3,000 to 2,400 cal yr BP) with high total Poaceae, a slight increase in Panicoideae and Asteraceae towards the end of the zone. The tree shrub

https://doi.org/10.5194/egusphere-2026-6376
Preprint. Discussion started: 23 November 2026
© Author(s) 2026. CC BY 4.0 License.

component declines and Arecaceae phytoliths appear at 2,500 cal yr BP. Woody phytoliths decline sharply around 2,350-2,000 cal yr BP, marked by a forest cover disturbance event (FCPE1, Fig. 5) and a concomitant decline in Asteraceae. Simultaneously, Cyperaceae, Panicoideae, Bambusoideae, and Poaceae increase. Arboreal phytoliths increase around 2,010 cal yr BP, followed by significant levels of Asteraceae, Panicoideae, and Bambusoideae. Arecaceae appears prominently at 1,800 cal yr BP. Morphological phytolith abundances similar to maize appear around 2,100 cal yr BP and disappear at the end of the zone at 1,740 cal yr BP (Table B1). A second FCPE appears at 1,700 cal yr BP (Fig. 5), coinciding with a decrease in Asteraceae and a slight increase in Poaceae, Bambusoideae, and Chloridoideae phytoliths. In addition, the subfamily Panicoideae peaks between 1,100 and 670 cal yr BP. Maize phytoliths reappear at 1,200 cal yr BP and persist until 500 cal yr BP. Around this last date, Arecaceae phytoliths disappear and Bambusoideae show a marked decline, a trend that continues into the early 20th century.

A significant recovery of woody phytoliths, along with Bambusoideae, Asteraceae, and Cyperaceae, begins in the 20th century and peaks toward the end of the sequence. In modern times (c. 2000 CE), "arboreal" phytoliths, Asteraceae, and Cyperaceae peak, accompanied by a slight decline in Panicoideae, Bambusoideae, Chloridoideae, and Stipa. In particular, Poaceae phytoliths show a marked decrease.

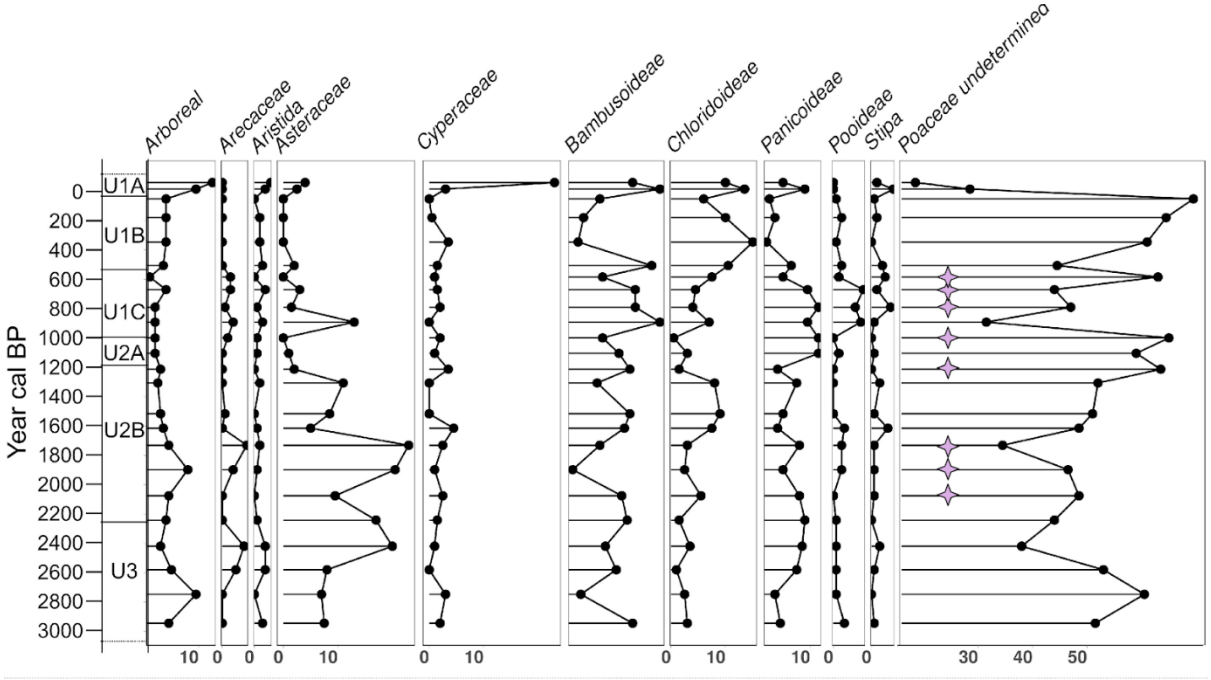

Fig. 4. Phytolith percentage diagram from the compiled Lake Vichuquén sedimentary record.
The presence of maize phytoliths is indicated in purple diamonds within the category of Poaceae. Boxes on the left show the stratigraphic units.

https://doi.org/10.5194/egusphere-2026-6376
Preprint. Discussion started: 23 November 2026
© Author(s) 2026. CC BY 4.0 License.

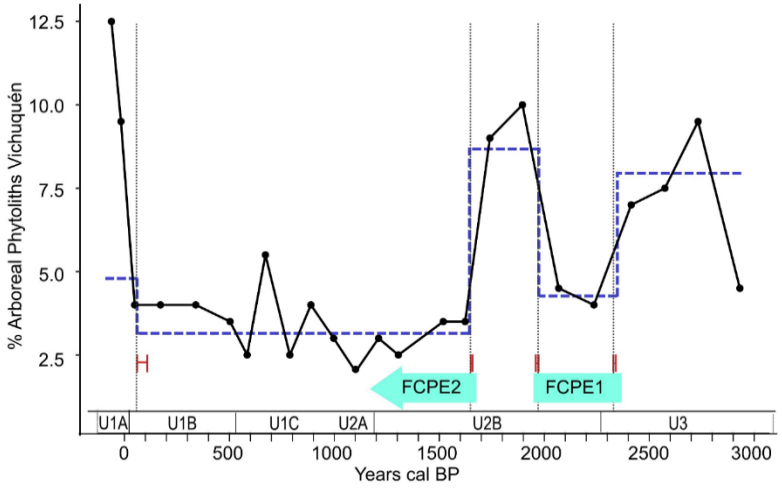

Fig. 5. Changepoint analysis of arboreal phytoliths from Lake Vichuquén over the last 3000 cal yr BP.

Significant decreases in tree-scrub cover are observed twice in the compiled Vichuquén sedimentary cores, first c. 2,350 cal yr BP (FCPE1) and a second event around 1,700 cal yr BP (FCPE2). Later there is a significant increase in historical times. The blue dashed line describes the points of significant changes detected by the R package Changepoint (Killick and Eckley, 2014) and red bars show the confidence interval (95%) for each change point detected. Boxes on the left show the stratigraphic units.

4.4 Vegetation dynamics inferred from pollen analyses

The pollen record from Lake Vichuquén spans approximately the last 3,000 cal yr BP and is divided into two main zones (C2 and C1; Fig. 6). The assemblage is generally dominated by non-arboreal pollen (NAP), particularly herbaceous taxa such as Poaceae, Chenopodiaceae, and various Asteraceae, with marked changes through time in the representation of arboreal, shrub, and herbaceous pollen taxa. Arboreal and shrub pollen taxa include *Nothofagus* spp., *Podocarpus*, *Myrceugenia* type, *Quillaja*, Lithraea, and *Baccharis* type, among others. *Nothofagus* dombeyi type and *Podocarpus*, which occur at low abundances throughout the sequence, are considered to represent long-distance pollen transport rather than local vegetation. In the most recent part of the record, Pinus appears together with *Rumex* type, indicating increasing anthropogenic influence associated with land-use changes around the lake.

Zone C2 (Subzones C2c, C2b, C2a). Between ca. 3,000 and 1,300 cal yr BP, NAP reaches its highest representation in the sequence. The oldest subzones (C2c and C2b) are characterized by low arboreal pollen representation and high abundances of herbaceous taxa, particularly Poaceae and Chenopodiaceae, together with Apiaceae (*Mulinum* type) in C2c and Asteraceae (*Leucheria* type) in C2b. Towards subzone C2a, the pollen assemblage becomes more diverse, with a slight increase in *Nothofagus obliqua* type and the continued presence of *Leucheria* type, together with an increased representation of other arboreal, shrub, and herbaceous taxa.

https://doi.org/10.5194/egusphere-2026-6376
Preprint. Discussion started: 23 November 2026
© Author(s) 2026. CC BY 4.0 License.

Zone C1 (Subzones C1c, C1b, C1a): The transition to Zone C1 is marked by a pronounced change in the AP/NAP index and in the relative representation and richness of arboreal, shrub, and herbaceous pollen taxa. During subzones C1c and C1b, several native arboreal and shrub pollen taxa increase in representation, including Lauraceae, *Baccharis* type, *Myrceugenia* type, *Adenopeltis* type, *Colliguaja* type, and *Aristotelia* type. *Nothofagus dombeyi* type and *Podocarpus* also occur during this interval but are interpreted as reflecting long-distance pollen transport. These changes coincide with a decline in Poaceae and the occurrence of herbaceous Asteraceae such as *Werneria* type and *Senecio* type. At the onset of C1c, aquatic and marsh taxa, particularly Cyperaceae and Typha, increase, together with ferns such as *Histiopteris*, indicating an expansion of aquatic or marsh vegetation. The most recent subzone (C1a) shows a marked change in pollen composition. Native arboreal and shrub pollen taxa such as *Myrceugenia* type, *Adenopeltis* type, and *Aristotelia* type remain represented, while Poaceae and *Plantago* increase and Chenopodiaceae decreases. Toward the uppermost part of the record, Pinus pollen becomes prominent together with *Rumex* type, reflecting increasing anthropogenic disturbance. *Muehlenbeckia* type is also recorded during this interval but is treated as a native component of the vegetation rather than as an exotic or disturbance indicator.

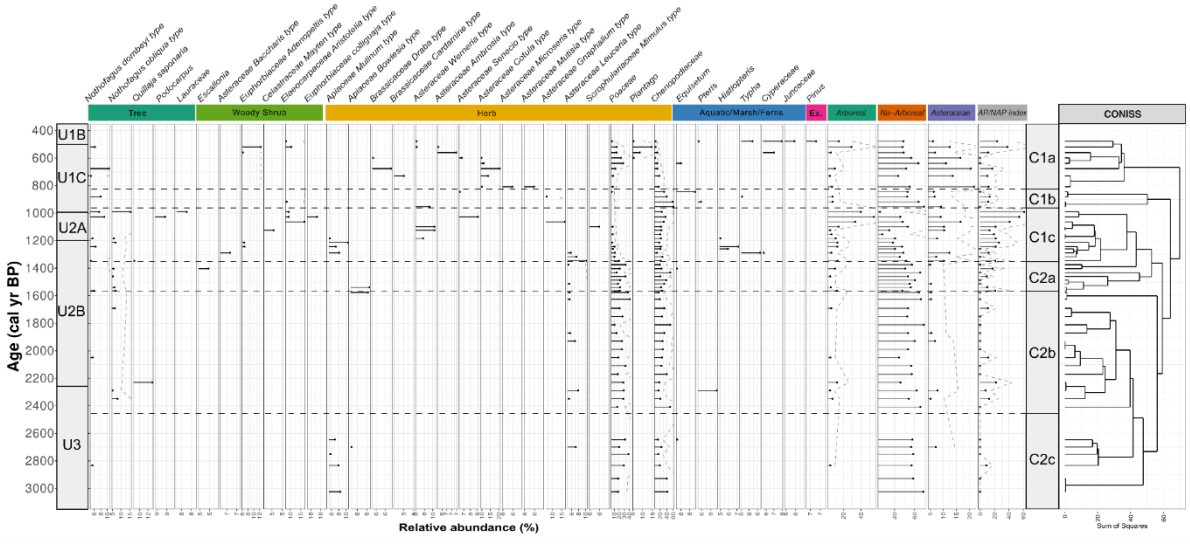

Fig. 6. Pollen diagram of the Lake Vichuquén composite sequence.

The diagram displays the most abundant taxa (≥5% relative abundance) plotted against age (cal yr BP) alongside corresponding lithostratigraphic units (U3–U1B). Summary panels on the right display variations in Arboreal Pollen (AP), Non-Arboreal Pollen (NAP), total Asteraceae, and the AP/NAP index. Local pollen assemblage zones (C2c to C1a) were statistically delineated using a stratigraphically constrained cluster analysis (CONISS)

4.5 Spectral and continuous wavelet analysis of hydroclimatic forcing and fire regimes

The wavelet analysis of the charcoal record distinguishes long-term biomass availability from short-term fire recurrence. The unfiltered CHAR spectrum (Fig. 7a) captures low-frequency background dynamics, with variance strongly concentrated in

https://doi.org/10.5194/egusphere-2026-6376
Preprint. Discussion started: 23 November 2026
© Author(s) 2026. CC BY 4.0 License.

centennial-to-millennial bands between ca. 3,000 and 1,000 cal yr BP, indicating sustained regional fuel loads. Changepoint analysis of the charcoal accumulation series identified significant regime shifts at ~1,200, 1,560, 2,080, and 2,300 cal yr BP (Fig. B4a). Conversely, the high-pass filtered spectrum (Fig. 7b) resolves the temporal structure of discrete fire events, revealing a robust, quasi-decadal fire regime (10–20 year periodicities) operating continuously from ca. 3,000 to 1,200 cal yr BP. Futhermore, the REDFIT analysis resolved a significant ~10–11-year cycle exceeding the 99% confidence level against AR(1) red-noise background (Fig. A3a). This rhythmic recurrence is punctuated by transient intervals of reduced power at ca. 2,200–2,150, 1,700–1,600, and 1,200–1,100 cal yr BP. Notably, both the low-frequency background biomass signal and the cyclical high-frequency ignition patterns abruptly collapse after 1,200 cal yr BP, marking a permanent regime shift in regional fire dynamics.

Wavelet analysis of the Rb/Sr ratio, a geochemical proxy tracking water balance and marine incursions versus freshwater retention, separates baseline hydrochemistry from transient saline/evaporative excursions. The unfiltered spectrum (Fig. 7c) reveals significant low-frequency variance in centennial bands (200–500 years) between ca. 2,000 and 1,200 cal yr BP, reflecting prolonged shifts in baseline water balance or marine-estuarine connectivity. Conversely, the high-pass filtered spectrum (Fig. 7d) resolves discrete hydrochemical pulses, isolating a non-stationary regime dominated by interannual-to-decadal periodicities (2–16 years). Spectral analysis using REDFIT revealed prominent periodic components at ~10–11 and ~6–7 yr (>99% confidence level), as well as at ~4–5 yr (>95% confidence level), against the fitted AR(1) red-noise spectrum (Fig. A3d). This high-frequency variance intensifies after ca. 1,800 cal yr BP, peaking between ca. 1,500 and 1,200 cal yr BP. Subsequently, hydrochemical variability is markedly reduced between ca. 1,000 and 500 cal yr BP, punctuated by a distinct decadal pulse at ca. 400 cal yr BP, before exhibiting suppressed variance toward the present.

Concurrently, wavelet analysis of the K/Ti ratio isolates changes in hydroclimate energy, and grain-size sorting (coarse sand pulses vs. quiet-water clay settling). In the unfiltered spectrum (Fig. 7e), centennial-scale variance is largely absent or constrained within the cone of influence, demonstrating that baseline catchment runoff lacked stable long-term cyclicity throughout the late Holocene. Instead, the system is characterized by discrete, high-frequency hydrodynamic shifts, highlighted by a statistically significant multidecadal pulse (~70–90 years) centered at ca. 850–750 cal yr BP. The 4–20-year bandpass-filtered series (Fig. 7f) isolates discrete high-energy runoff events, resolving recurrent decadal pulses across the sequence (notably at ca. 2,700–2,600, 2,250–2,100, and 1,800–1,500 cal yr BP). Spectral analysis using REDFIT revealed prominent periodic components at ~4–5 yr (>99% confidence level), as well as at ~10–11 and ~7–8 yr (>95% confidence level), against the fitted AR(1) red-noise spectrum (Fig. A3c). This high-frequency regime culminates in a prominent intensification centered at ca. 1,000–900 cal yr BP (10–12-year periodicities)—indicative of repeated flash-flood events—followed by episodic decadal pulses between ca. 500 and 250 cal yr BP and marked attenuation toward the present. Taken together, the changepoint and spectral analyses reveal a divergence between charcoal accumulation and the hydroclimatic proxies after ca. 1,200 cal yr BP. While CHAR underwent an abrupt and persistent reduction in both magnitude and decadal-scale variability, Rb/Sr and K/Ti retained episodic variability at comparable timescales during the subsequent interval (Figs. 7 and B4).

https://doi.org/10.5194/egusphere-2026-6376
Preprint. Discussion started: 23 November 2026
© Author(s) 2026. CC BY 4.0 License.

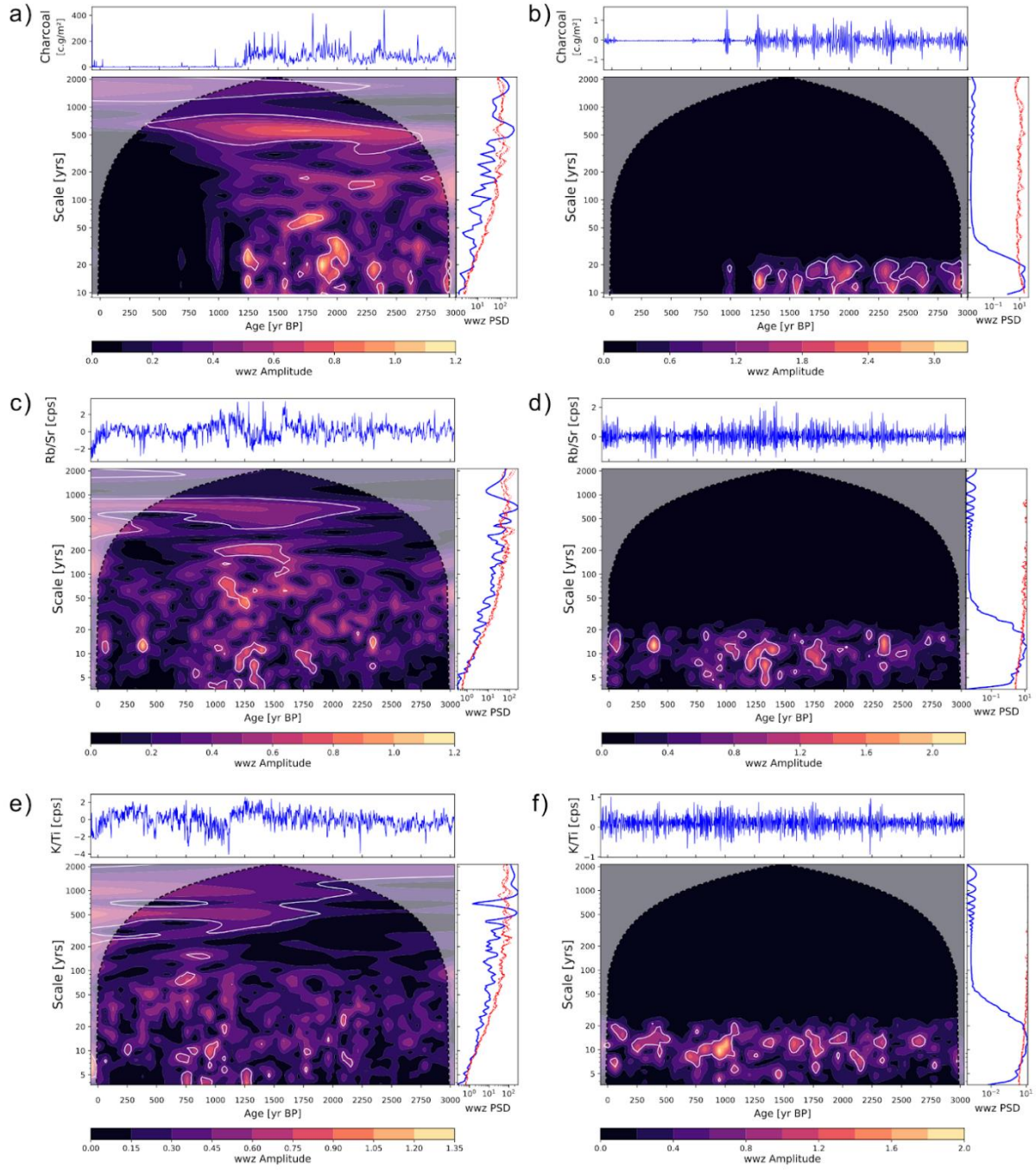

Fig. 7. Weighted Wavelet Z-transform (WWZ) spectral analysis of reconstructing fire frequency changes and decadal-scale terrestrial weathering history from the Lake Vichuquén sequence.

Panels display: (a) the original macroscopic charcoal time series and (b) its signal bandpass-filtered between 10 and 20 years; (c) the log-transformed Rb/Sr [cps] ratio and (d) its 4–20-year bandpass-filtered signal; (e) the log-transformed K/Ti

https://doi.org/10.5194/egusphere-2026-6376
Preprint. Discussion started: 23 November 2026
© Author(s) 2026. CC BY 4.0 License.

[cps] ratio and (f) its 4–20-year bandpass-filtered signal. For each proxy, the top section presents the time series, the lower-left section displays the WWZ amplitude scalogram, and the lower-right section shows the global Power Spectral Density (WWZ PSD). The horizontal axis represents age in years before present (Age [yr BP]), and the left vertical axis indicates the scale in years (Scale [yrs]). In the scalograms, solid contours enclose regions with significant confidence levels, whereas the PSD profiles explicitly indicate the 90%, 95%, and 99% confidence intervals (CI), calculated against a red-noise background. Shaded areas in the scalograms denote the cone of influence (COI), where wavelet edge effects compromise statistical significance.

4.6 Summed Probability Distribution

The Summed Probability Distribution (SPD) from the regional archaeological sites shows a gradual increase from approximately 2,500 cal BP, followed by a more pronounced rise after ~1800 cal BP and a first maximum around ~1,300 cal BP. The SPD subsequently declines, reaching a minimum around ~1,050–1,000 cal BP, before increasing again and attaining its highest values at approximately ~600 cal BP. Thereafter, summed probability progressively decreases toward the present.

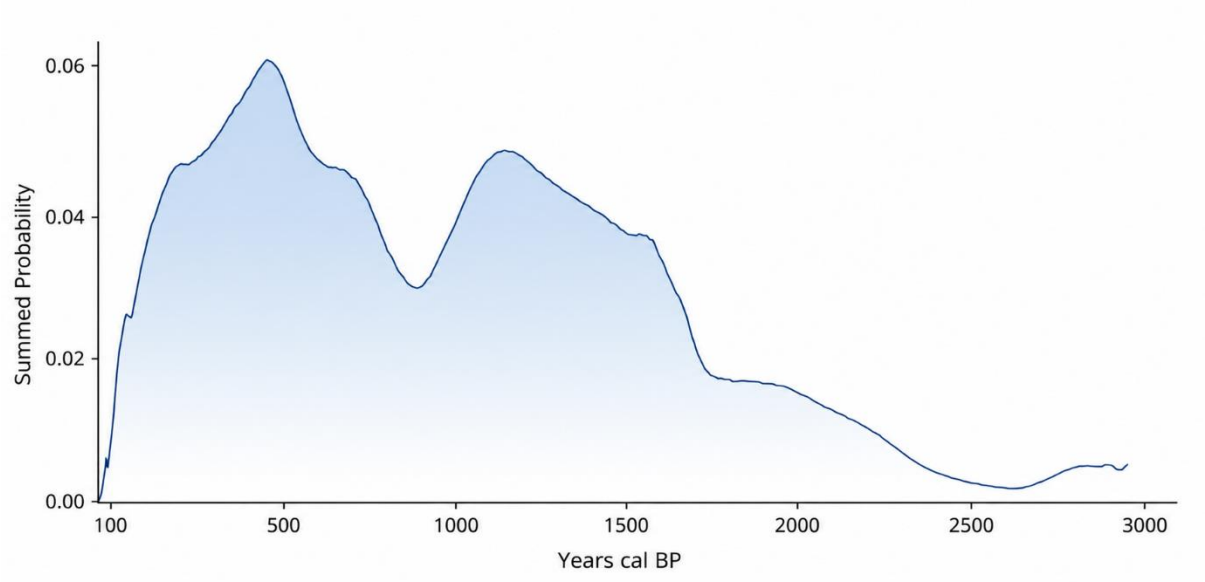

Fig. 8. Summed Probability Distribution (SPD) of 90 archaeological dates from 41 sites between 34.83° and 35.98°S in the Maule Region, central Chile.

5 Discussion

5.1 Climate drivers of fire regimes in central Chile

Our results indicate that fires were not only frequent in the Vichuquén Basin, but also a relevant landscape process with complex underlying natural variability, especially between 3,000 and 1,200 cal yr BP (Fig. 7). Several local and regional records show a strong intensification of ENSO-like activity and highlight a wetter climate than the present after 2,000 cal yr BP (Jenny et al., 2002; Frugone-Álvarez et al., 2017; 2020; Maldonado and Villagrán, 2006; Rein et al., 2005; Villa-Martínez et al., 2004; Villa-Martínez and Villagrán, 1997). Indeed, the Vichuquén record shows periods of increased

https://doi.org/10.5194/egusphere-2026-6376
Preprint. Discussion started: 23 November 2026
© Author(s) 2026. CC BY 4.0 License.

charcoal accumulation after 2,100 cal yr BP, coinciding with an increased influx of arboreal phytoliths (Fig. 5). Rather than a true canopy recovery, this concurrent increase of charcoal and arboreal phytoliths likely reflects enhanced erosion and transport of burned woody debris from the basin slopes, all relatively synchronous with an increase in regional ENSO-like activity (Figs 7 and 10).

Higher organic carbon accumulation in the lake and elevated C/N ratios (>12) of organic matter during 2,200–1,700 cal yr BP also indicate higher soil disturbance in the basin (Fig. 2). As a proxy for weathering and erosion processes in the basin, the Rb/Sr and K/Ti ratios show a similar PDO-ENSO type pattern since ca. 2,500 cal yr BP with a significant decadal variability, further supporting the natural cyclical component of these changes (Figs. 7 and A3c–d). Specifically, downcore Rb/Sr variations integrate catchment runoff dynamics and regional hydrological balance governed by mineral-specific fractionation; while Rb is sequestered within the crystal lattice of unweathered detrital muscovite and associated phyllosilicates delivered via fluvial runoff, Sr exhibits a dual partitioning (see Frugone-Álvarez et al., 2017). In the detrital fraction, Sr is hosted via isomorphous Ca^{+2} (substitution in plagioclase) but it becomes strongly enriched in authigenic calcite and evaporitic gypsum precipitated during low-stand evaporative stages and, possible marine-water incursions into the coastal lagoon (Units 3–2). Between 3,000 and 1,250 cal yr BP, low Rb/Sr values indicate reduced freshwater runoff and a negative basin water balance, where detrital dilution was overridden by the precipitation of calcite/gypsum. Notably, Rb/Sr ratios shift definitively toward maximum values (>1.0) after ca. 1,000 cal yr BP (Transition 1, ~200 cm depth), a threshold marked by the complete disappearance of calcite and gypsum in the mineralogical profile and the onset of steady, entirely freshwater sedimentation (~3.2 a cm^{-1}) (Frugone-Álvarez et al., 2017). Concurrently, elevated K/Ti values reflect enhanced delivery of physical detritus rich in muscovite relative to resistant titanium-bearing mineral residues, confirming high-energy mechanical erosion with minimal chemical leaching in the watershed (Bonk et al., 2016). The increase in the frequency and accumulation rates of fires over the past 2,500 years has occurred at times when the available biomass has been modulated in part by climatic factors (Figs. 7, 9 and 10). However, most of the identified fire events produced relatively low to moderate charcoal peaks compared with those recorded in the most recent part of the sequence, particularly the 2017 fire event.

The period with the highest charcoal input into Lake Vichuquén occurred between 1,500 and 1,380 cal yr BP, with fires of medium magnitude and high frequency (Fig. 3). This is associated with increased moisture conditions and strong ENSO-like interannual variability at regional and local scales (Figs. 7, 9 and A3) (Jenny et al., 2002; Villa-Martínez et al., 2004), which is also supported by the marked interannual variability of erosion proxies in Vichuquén in this time window (Fig. 7c-d). This wet period with a marked ENSO-PDO tendency, could have facilitated the accumulation and connectivity of fuel for ignition between alternating very wet and very dry seasons.

https://doi.org/10.5194/egusphere-2026-6376
Preprint. Discussion started: 23 November 2026
© Author(s) 2026. CC BY 4.0 License.

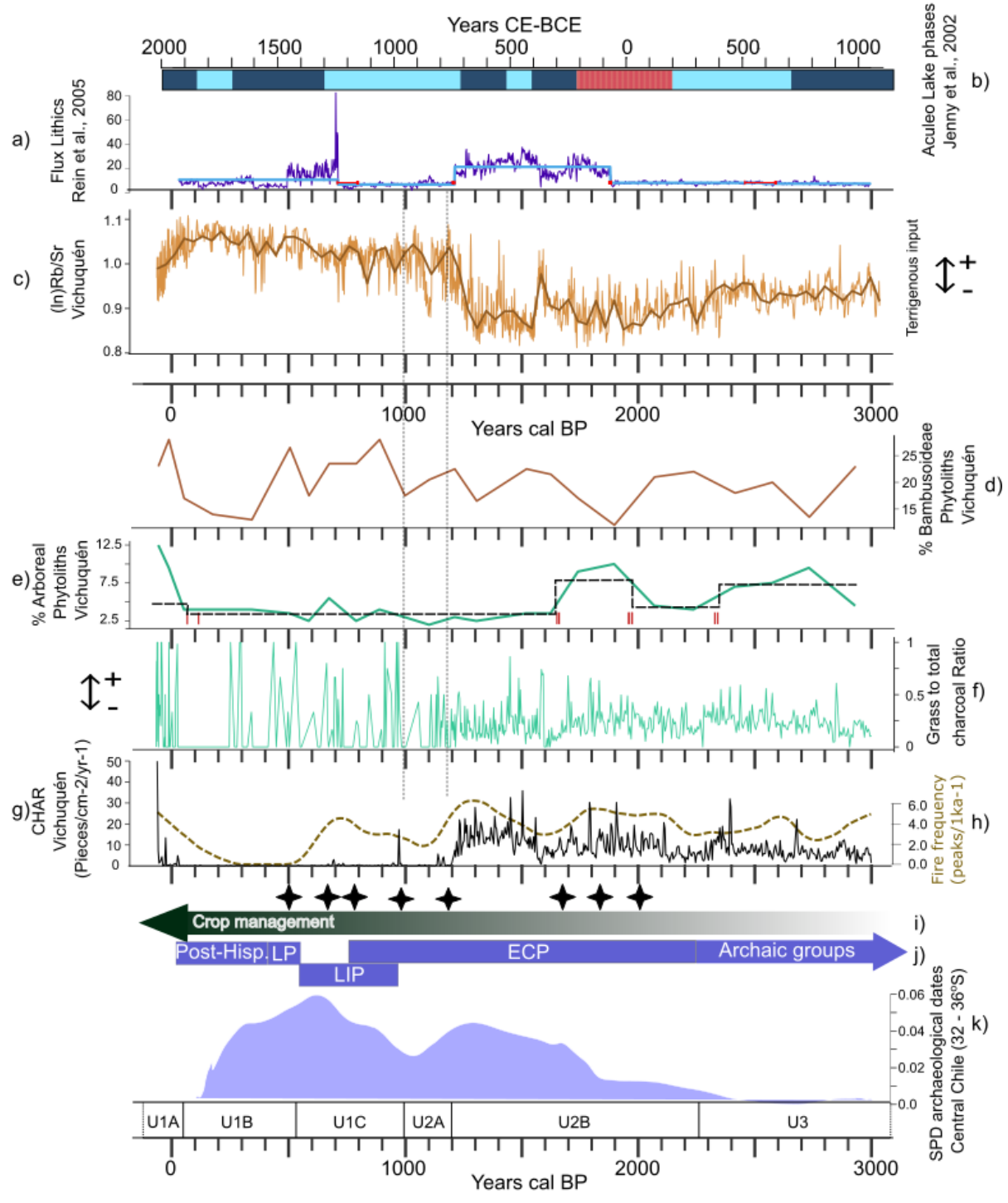

Fig. 9. Summary of the Lake Vichuquén record and regional comparative data.

https://doi.org/10.5194/egusphere-2026-6376
Preprint. Discussion started: 23 November 2026
© Author(s) 2026. CC BY 4.0 License.

a) Lithic flux from the marine sediment core off Lima, used as a proxy for ENSO variability (Rein et al., 2005). b) Schematic representation of Laguna Aculeo lake phases: light blue indicates wetter conditions, red hatching indicates drier conditions, and dark blue indicates phases of increased flooding (Jenny et al., 2002). c) ln(Rb/Sr) ratio from Lake Vichuquén (Frugone-Álvarez et al., 2017). d) Percentage of Bambusoideae phytoliths from Lake Vichuquén. e) Percentage of arboreal phytoliths from Lake Vichuquén. f) Grass-to-total charcoal ratio. g) Macroscopic charcoal accumulation rate (CHAR; particles cm^{-2} yr^{-1}) from Lake Vichuquén. h) Fire frequency reconstructed from the Lake Vichuquén charcoal record. i) Qualitative representation of changes in crop management intensity in central Chile. Black stars indicate levels containing cf. *Zea mays* phytoliths in the Lake Vichuquén sequence. j) Archaeological periods of central Chile: Archaic groups, Early Ceramic Period (ECP), Late Intermediate Period (LIP), Late Period (LP), and Post-Hispanic period. k) Summed Probability Distribution (SPD) of 90 available archaeological dates from 41 sites in the Maule Region (34.83–35.98°S). Vertical dotted lines indicate the sedimentary subunit associated with the closure of the Vichuquén basin.

.

The large decrease in charcoal accumulation rates (c. 1,200-1,250 cal yr BP) is coeval with other changes in the Lake Vichuquén sedimentary record. After c. 1200 cal yr BP, the geochemical proxies show a substantial increase in the transport of highly weathered soil particles into the lake which persists to the present (Figs. 7c–e and 9c). Biogeochemical proxies distinctly demarcate transition T1 (ca. 1,000 cal yr BP; ~200 cm depth; Figs. 2 and A2), where declining atomic C/N ratios (<9) and more negative $\delta^{13}C$ values (ca. -25‰ and -26‰) across the U2A/U1C boundary reflects the cessation of marine-brackish inputs and confirms the establishment of an autochthonous freshwater phytoplankton regime in a closed lacustrine basin. At the same time, geochemical proxies indicate that the transport of catchment-derived material continued after the transition (Figs. 7c–e and 9c). Along this transition towards reduced connectivity with the ocean, a slight increase in $\delta^{15}N$ values occurs (Fig. 2d). Increased $\delta^{15}N$ values in central Chilean lake sediments have previously been associated with enhanced nutrient inputs from the watershed during periods of reduced vegetation cover (Fuentealba et al., 2020, 2021). In this context, the increase observed at Vichuquén may reflect enhanced terrestrial nutrient inputs associated with greater watershed disturbance. Although this reorganization of the lake system may have affected charcoal transport and deposition, several observations indicate that it cannot by itself account for the magnitude and persistence of the decline in CHAR. No concomitant abrupt change in sedimentation rate is observed (Fig. A2). Moreover, the same closed-lake system subsequently records a recovery in CHAR during the 20th century and a pronounced peak associated with the January 2017 megafire. These observations argue against interpreting the post-ca. 1,200 cal yr BP decline in CHAR as an exclusively depositional response to basin closure. Importantly, this transition involves not only a reduction in charcoal accumulation but also a reorganization of its temporal variability, as revealed by the changepoint and spectral analyses (Figs. 7 and B4). Several records from central Chile and surrounding regions indicate decreased ENSO-like activity around 1,200–1,000 cal yr BP (Jenny et al., 2002; Rein et al., 2005; Moy et al., 2002; Maldonado and Villagrán, 2006). Prior to ca. 1,200–1,000 cal yr BP, macrocharcoal exhibited pronounced decadal-to-interdecadal variability, with episodic significant coherence with the regional ENSO-related marine record (Fig. 10), alongside periodicities comparable to those identified in the local hydroclimatic proxies (Figs. 7 and A3). After this interval, this signal is no longer evident in the charcoal record, whereas

https://doi.org/10.5194/egusphere-2026-6376
Preprint. Discussion started: 23 November 2026
© Author(s) 2026. CC BY 4.0 License.

Rb/Sr continues to show subdecadal variability until ca. 650 cal yr BP and again between ca. 450 and 250 cal yr BP. This divergence is particularly evident between ca. 450 and 250 cal yr BP, when subdecadal variability reappears in the Vichuquén erosion proxies (K/Ti and Rb/Sr) and other regional records document increased occurrence of torrential rainfall events, without a comparable recovery in CHAR (Jenny et al., 2002). Because this divergence occurs well after the establishment of fully lacustrine conditions, it cannot be explained simply by the initial transition from a coastal lagoon to a closed lake. Instead, it indicates that the contrasting behavior of charcoal and hydroclimatic proxies persisted within the subsequent lacustrine system. This suggests that the relationship between hydroclimatic variability and fire activity changed during the later part of the sequence, and that climatic conditions that had previously favored fire did not necessarily produce an equivalent fire response thereafter.

At a broader spatial scale, the available microcharcoal records indicate that fire histories across central Chile were heterogeneous rather than strictly synchronous (Fig. 11). Nevertheless, several records, including Matanzas, Chepical, and Laguna de Tagua Tagua, show decreases in charcoal accumulation broadly within the ca. 1,300–1,000 cal yr BP interval, although they differ in the precise timing, magnitude, and proposed causes of these changes. This spatial variability is also reflected in the different explanations proposed for individual records. At Matanzas, the charcoal decline has been related to possible changes in human occupation associated with shifting dune ridges along the central coast (Villa-Martínez, 2002). At Chepical, in contrast, it has been attributed to reduced biomass and drier conditions in the lower valleys (Martel-Cea et al., 2016), whereas reduced moisture availability has also been proposed to explain the trajectory at Laguna de Tagua Tagua, in agreement with its pollen record (Heusser, 1983). Lake Aculeo further illustrates this spatial heterogeneity: it does not show a comparable decline around 1,200 cal yr BP, but instead displays relatively low and variable CHAR values followed by several later increases, particularly during the last ca. 500 years (Fig. 11c; Villa-Martínez, 2002). Thus, the regional records do not indicate a synchronous and uniform shift in fire activity, but rather spatially heterogeneous responses to environmental and possible socioecological changes during the late Holocene.

https://doi.org/10.5194/egusphere-2026-6376
Preprint. Discussion started: 23 November 2026
© Author(s) 2026. CC BY 4.0 License.

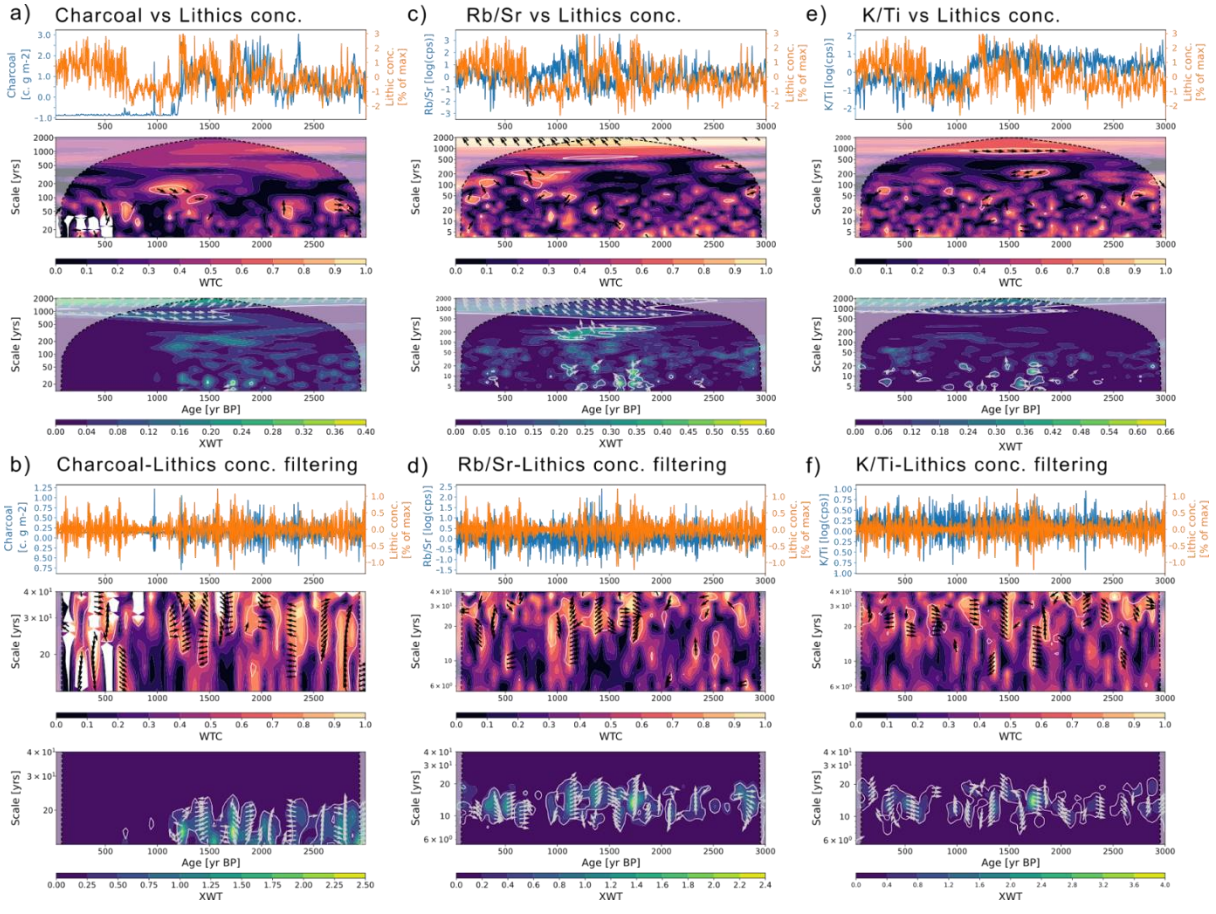

Fig. 10. Cross-wavelet transform (XWT) and wavelet coherence (WTC) analysis between fire/weathering proxies from the Lake Vichuquén sequence and lithic concentrations from the 106KL marine sedimentary record off the Peruvian coast (Rein et al., 2005). Panels show the relationships for (a) Original macroscopic charcoal vs. lithic concentrations [% of maximum] and (b) their 10–20 year bandpass-filtered signals; (c) log-transformed Rb/Sr ratio vs. lithic concentrations [% of maximum] and (d) their 4–20-year bandpass-filtered signals; (e) log-transformed K/Ti ratio vs. lithic concentrations and (f) their 4–20-year bandpass-filtered signals. For each proxy pair: The top section presents the standardized time series, where the proxy is shown in blue and the lithic concentration in orange. The middle section displays the WTC scalogram, illustrating local correlation in time-frequency space. The bottom section shows the XWT power scalogram, highlighting common regions of high power. The horizontal axis represents the age in years before present, and the vertical axis indicates the oscillation scale in years (Scale [yrs]). Arrows indicate phase relationships between co-analyzed time series. Right-pointing arrows (→) denote in-phase oscillations; left-pointing arrows (←) indicate anti-phase (180°) relationships; upward arrows (↑) represent a 90° phase lead in the second time series; and downward arrows (↓) indicate a 90° phase lag. Thick black contours enclose regions of wavelet coherence/power exceeding the 95% significance threshold, calculated against a red-noise null model. Shaded areas denote the cone of influence (COI), where edge effects compromise statistical significance.

5.2 Socio-ecological drivers of fire regime changes

Phytolith data suggest that the areas surrounding Lake Vichuquén experienced two distinct episodes of vegetation opening: FCPE1 at ca. 2,400 cal yr BP and FCPE2 at ca. 1,700 cal yr BP (Figs. 5 and 9). Prior to FCPE1, the higher abundance of

https://doi.org/10.5194/egusphere-2026-6376
Preprint. Discussion started: 23 November 2026
© Author(s) 2026. CC BY 4.0 License.

woody phytoliths indicates a greater local representation of woody vegetation. Following FCPE1, arboreal components decline and indicators of landscape openness associated with understory and ruderal taxa increase (Giraldo-Cañas et al., 2012; Reid et al., 2004). A similar, and more pronounced, signal occurs at ca. 1,700 cal yr BP during FCPE2 (Fig. 9d–h). Both episodes coincide with increased input of woody components to the sedimentary record, particularly FCPE2 (Fig. 9e). Although several regional paleoclimate records suggest relatively wet conditions during this interval, the multiproxy evidence from Lake Vichuquén reveals a progressive aridification trend that intensified toward transition T1 (ca. 1,000 cal yr BP). Consequently, a sustained negative water balance and catchment-scale desiccation emerge as plausible primary drivers of these vegetation-opening episodes, overriding broader regional generalizations (Frugone-Álvarez et al., 2017, 2020; Jenny et al., 2002; Maldonado and Villagrán, 2002; Villa-Martínez, 2002; Villa-Martínez et al., 2003; Villagrán and Varela, 1990). FCPE1 coincides with a period of accelerated per capita population growth at the regional scale between ca. 2,600 and 2,400 cal yr BP (Gayó et al., 2019; Godoy-Aguirre et al., 2024), while the Maule SPD begins to increase gradually from ca. 2,500 cal yr BP (Fig. 9k). Human presence in the Vichuquén area predates FCPE1, as shown by an individual burial dated to ca. 3,000 cal yr BP (Cornejo, 1988), although this earlier evidence does not establish that FCPE1 led to more semipermanent occupations.

Maize is recorded in the Vichuquén basin between ca. 2,100 and 1,740 cal yr BP (Fig. 4), indicating the establishment of horticultural practices during this interval. Its appearance coincides with a period of increased ENSO-like hydroclimatic variability (Figs. 7, 9, 10 and A3), in a context comparable to the development of early horticulture documented elsewhere in central Chile (Sanhueza, 2013). Following FCPE2, the archaeological record shows an increase in both the number of sites and the intensity of occupations associated with the local onset of the Early Ceramic Period (Rees et al., 1993a, 1993b; Seelenfreund et al., 1991; Seelenfreund, 1995). The Maule SPD likewise shows a pronounced increase after ca. 1,800 cal yr BP (Fig. 9k). This increase in archaeological activity occurs during the same interval in which CHAR rises following FCPE2 and remains elevated until the abrupt change in the fire record at ca. 1,250–1,200 cal yr BP (Fig. 9g–h).

The period after ca. 1,250–1,200 cal yr BP marks an important reorganization of the socio-ecological system at Vichuquén. After ca. 1,200 cal yr BP, settlements gradually shifted toward areas with greater potential for irrigation, expanding beyond traditional rainfed horticultural strategies (Falabella et al., 2015). On the Maule coast, archaeological sites reach high frequencies after ca. 1,100 cal yr BP (Aldunate et al., 1991; Rees et al., 1995). At Vichuquén, maize phytoliths remain present after ca. 1,200 cal yr BP, while isotopic evidence from the Maule Valley shows increased C4 plant consumption between ca. 1,070 and 790 cal yr BP (Correa and Carrasco, 2017) (Figs. 4 and 9). The marked decline in CHAR after ca. 1,200 cal yr BP does not appear to coincide with a decline in horticultural practices or archaeological activity in the region.

The regional vegetation dynamics inferred from the Vichuquén pollen record provide a critical spatial counterpart to the local phytolith and macroscopic charcoal records, offering an independent proxy to evaluate the late Holocene fire-vegetation-climate-human interactions (Fig. 6). Prior to ~1,200 cal yr BP (Zones U3/C2c and U2B/C2b), the low abundance of arboreal and shrub pollen taxa (Lauraceae, Quillajaceae, Lithraea, *Myrceugenia*, *Baccharis*) and the clear dominance of Chenopodiaceae and Poaceae, together with heliophytic herbs (*Mulinum*, *Leucheria*), are consistent with relatively open

https://doi.org/10.5194/egusphere-2026-6376
Preprint. Discussion started: 23 November 2026
© Author(s) 2026. CC BY 4.0 License.

vegetation. *Nothofagus dombeyi* type and *Podocarpus* are interpreted as long-distance pollen inputs and are therefore not used to infer local vegetation. The marked compositional shift observed after ~1,200 cal yr BP—which partly coincides with the transition to a more closed lacustrine basin (Unit/Zone 2U/C1c)—is clearly captured by the palynological record (Fig. 6). Herbaceous taxa declined between ca. 1,300 and 800 cal yr BP, followed by increasing representation of shrub pollen taxa, including Asteraceae *Baccharis* type, Euphorbiaceae *Adenopeltis* and *Colliguaja* types, and Eleocarpaceae *Aristotelia* type. Shallow-water and marsh-associated taxa, including *Typha* and Hysteopteris, also increased, potentially reflecting an expansion of shallow-water areas or lower lake levels. This interval partly overlaps with the Medieval Climate Anomaly (MCA; ca. 1,200–850 cal yr BP), while the increase in Chenopodiaceae between ca. 1,000 and 800 cal yr BP (Zone C1b) is consistent with increased aridity during part of this period.

The decline in CHAR after ca. 1,200 cal yr BP therefore coincided with this reorganization of vegetation, but not with a comparable decline in human activity. Maize phytoliths persisted in the Vichuquén record, while archaeological evidence indicates continued occupation and horticultural activity in the Maule region (Fig. 9). The high fire activity that had broadly accompanied the earlier expansion of horticulture and archaeological activity was thus no longer maintained during the later phase.

Rather than indicating a simple reduction in anthropogenic burning, this divergence may reflect a change in the relationship among human activity, vegetation, and fire after ca. 1,200 cal yr BP. Changes in vegetation composition may have altered the availability and spatial distribution of fuels while archaeological activity in the region continued. The resulting fire regime may therefore have depended on the interaction between human activity and the ecological configuration of a changing landscape. Such nonlinear relationships between land use, vegetation, and fire have been documented in historical-ecological approaches to anthropogenic fire regimes (Bowman et al., 2011; Roos et al., 2014).

Historical accounts from south-central Chile indicate that the relationship between agricultural land use and fire was neither necessarily proportional nor constant through time. Reche-Mapuche communities used fire for clearing and cultivation but also preferentially reused previously cleared areas (Delgado, 2016; Godoy, 2008). Other historical sources document episodes of more extensive land clearance and the use of fire in vegetation and agricultural management (Bullock, 1911; de Vivar, 1558; González de Nájera, 1614; Maas, 1847; Smith, 1914). Although these historical practices cannot be directly extrapolated to the earlier Vichuquén sequence, they show that sustained agricultural activity could occur under different patterns of fire use. The Vichuquén record shows a comparable non-linear relationship: after ca. 1,200–1,000 cal yr BP, horticultural practices persisted and archaeological activity remained high while charcoal accumulation was substantially lower than during the preceding interval. Low CHAR also persisted during the progressive weakening of interannual-to-subdecadal hydroclimatic variability between ca. 950 and 650 cal yr BP and a relatively warm interval broadly coeval with the MCA in central Chile (Von Gunten et al., 2009). Fire activity during this period therefore developed under changing conditions of both land use and hydroclimate, rather than tracking either factor in a simple or proportional way.

Human settlement expanded across central Chile during the Inka state (Late Period, ca. 550–400 cal yr BP), accompanied by agricultural intensification and the expansion of irrigation systems (Gayó et al., 2019; Uribe and Sánchez, 2016; Stehberg et

https://doi.org/10.5194/egusphere-2026-6376
Preprint. Discussion started: 23 November 2026
© Author(s) 2026. CC BY 4.0 License.

al., 2021). Archaeological and ethnohistorical evidence indicates an Inka presence at Vichuquén, including mitimaes, followed by the incorporation of the area into the Spanish colonial system during the 16th century (Frugone-Álvarez et al., 2018; Guevara, 1997; León Echaiz, 1957; Odone, 1998). During this interval, Bambusoideae phytoliths begin a sustained decline, cf. *Zea mays* phytoliths persist until ca. 500 cal yr BP, and terrigenous-input proxies increase markedly (Fig. 7). The Maule SPD reaches its highest values at ca. 600 cal yr BP (Fig. 9k), indicating particularly high archaeological activity immediately before and around the onset of the Late Period (Inka presence). Despite this intensification of land use and occupation, CHAR remained low relative to the earlier pre-ca. 1,200 cal yr BP phase.

The transition to the Colonial Period at ca. 410 cal yr BP (1541 CE) was accompanied by further changes in the Vichuquén basin. Bambusoideae phytoliths declined markedly and Arecaceae phytoliths disappeared around ca. 500 cal yr BP, while Br/Ti and Rb/Sr record changes in lacustrine productivity and catchment-derived sediment input during this transition (Fig. 9). Changes in $\delta^{15}N$ provide additional evidence of altered nutrient dynamics within the basin. At the same time, subdecadal variability reappears in the Rb/Sr record between ca. 450 and 250 cal yr BP (Fig. 7). This renewed hydroclimatic variability was not accompanied by a comparable recovery in CHAR: fire frequency reached its lowest values between ca. 500 and 300 cal yr BP, while charcoal accumulation remained low. The Late-to-Colonial transition therefore extends the post-ca. 1,200 cal yr BP pattern, with substantial environmental and land-use changes occurring without a return to the high charcoal accumulation characteristic of the earlier part of the sequence.

Tree-ring fire-scar records from the Cachapoal basin document a shift in fire activity between 1541 and 1750 CE (ca. 409–200 cal yr BP), interpreted as evidence for increased fire use in land clearing, agriculture, and ranching (Rozas et al., 2018). At Vichuquén, fire frequency also begins a sustained increase after ca. 300 cal yr BP, including during the 17th century, but this increase is not accompanied by a comparable rise in CHAR or peak magnitude. The contrast between more frequent fire episodes and persistently low charcoal accumulation indicates that the historical increase in fire frequency did not recreate the fire regime recorded during the earlier prehispanic phase. This distinction becomes particularly important in the 20th century, when both vegetation composition and charcoal accumulation change sharply.

https://doi.org/10.5194/egusphere-2026-6376
Preprint. Discussion started: 23 November 2026
© Author(s) 2026. CC BY 4.0 License.

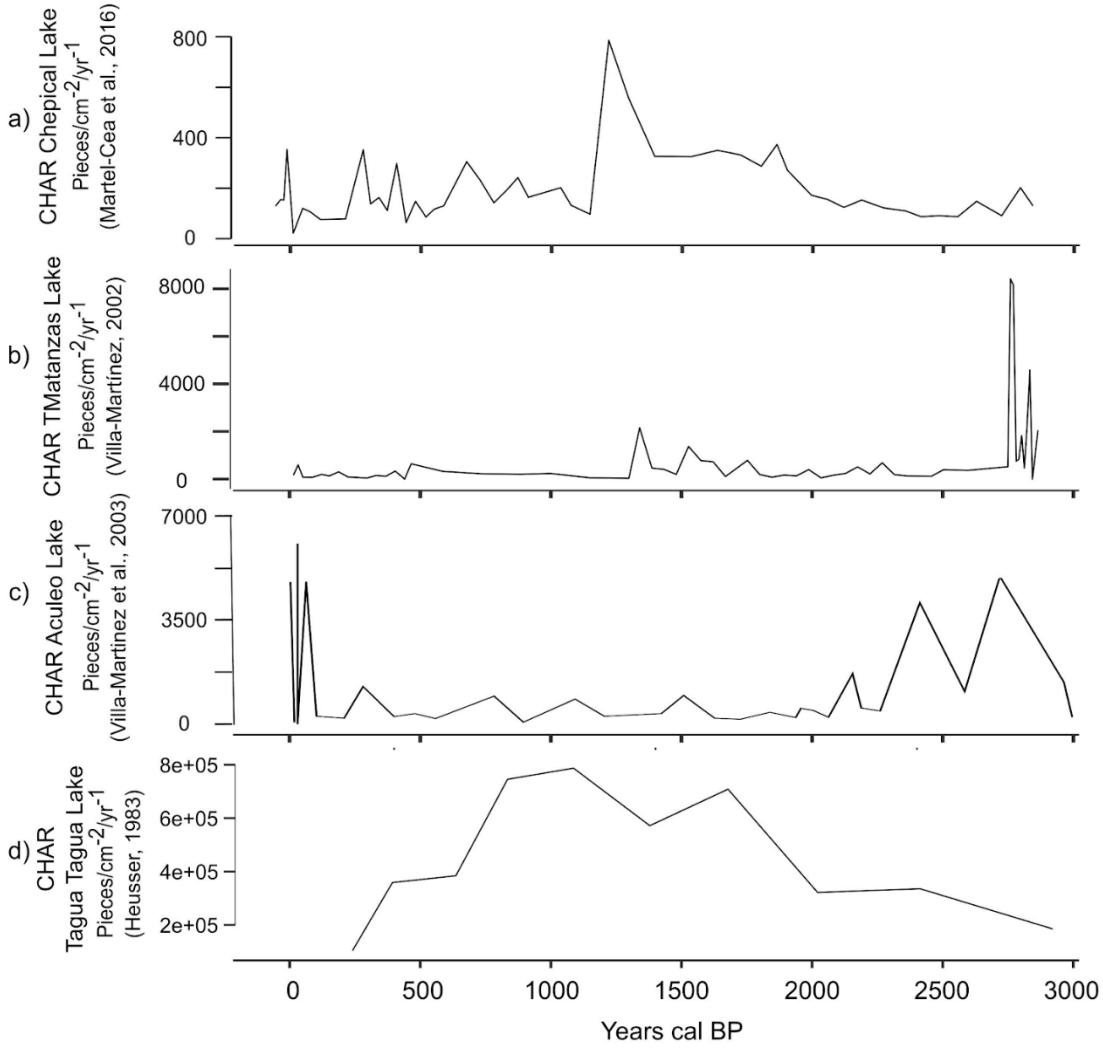

Fig. 11. Summary of microcharcoal (CHAR: particles cm^{-2} yr^{-1}) records from lacustrine sedimentary sequences in central Chile.

5.3 A new fire regime in the 20th century?

The pollen assemblage in the most recent layer (facies 1A, after 1880 CE) clearly indicates a marked change in regional vegetation composition. The marked increase in exotic *Pinus* pollen, together with *Rumex* type, is consistent with the historical expansion of commercial timber plantations and intensified land use in the basin. *Muehlenbeckia* type is also present but is considered a native component of the vegetation rather than an exotic or disturbance indicator. This modern palynological shift mirrors the recovery of arboreal phytoliths but reflects a distinct vegetation configuration compared to the pre-1,200 cal yr BP period. The introduction and massive expansion of highly flammable exotic monocultures (*Pinus*) likely increased landscape-level fuel connectivity, with greater vertical and horizontal biomass continuity than the native sclerophyllous mosaic. This contemporary accumulation of homogeneous, highly connected fuel provided the critical

https://doi.org/10.5194/egusphere-2026-6376
Preprint. Discussion started: 23 November 2026
© Author(s) 2026. CC BY 4.0 License.

structural prerequisites that, combined with 21st-century extreme climate variability and droughts, contributed to the catastrophic megafire regimes currently observed in central Chile.

While fire frequency increased in the prehistoric and colonial periods, charcoal accumulation increased significantly in the early and late 20th century (covered by 31 samples in the record). The second half of the 20th century witnessed a concomitant increase in tree phytoliths due to exotic tree plantations (*Pinus radiata*; *Eucalyptus globulus*) exploited for timber, which altered nutrient cycles in Vichuquén (Fuentealba et al., 2020, 2021). The abundance of tree phytoliths peaked in the last decade. The largest recorded fire event in the last 3,000 years occurred in January 2017, burning over 500,000 ha in south-central Chile (Pliscoff et al., 2020). These changes, coupled with a new climate regime and a widespread "megadrought" since 2010 in central Chile (Garreaud et al., 2017), suggest the onset of a new fire regime associated with accelerated anthropic modification of the vegetation landscape.

6 Conclusions

The Vichuquén sedimentary record demonstrates that fire was an important component of landscape dynamics in central Chile well before European colonization, challenging the characterization of this region as historically “fireless.” Fire activity, however, was far from constant, showing marked changes and variability throughout the 3,000-year sequence. Prior to ca. 1,200 cal yr BP, charcoal variability was closely associated with decadal-to-interdecadal hydroclimatic variability consistent with ENSO/PDO-like dynamics. Fire activity increased during a period of growing archaeological activity at the regional scale, possible episodes of landscape opening, and the beginning of horticultural practices in central Chile. These patterns raise the possibility that human land use also played a role in the prehispanic fire regime, alongside climate variability, although clarifying the extent and timing of this influence will require additional high-resolution local records from multiple sites.

After ca. 1,200–950 cal yr BP, this relationship changed substantially. Charcoal accumulation declined and its previous hydroclimatic variability disappeared, while horticultural practices persisted and regional archaeological activity remained high. Fire activity therefore became increasingly decoupled from the relationships observed during the earlier part of the record. A further reorganization occurred during the 20th century, when the expansion of exotic tree plantations, increasing woody vegetation, and prolonged drought coincided with a marked recovery in charcoal accumulation and the emergence of the modern fire regime.

The exceptional character of the 2017 event shows that the modern fire regime has no clear analogue within the previous three millennia at Vichuquén. More broadly, the record indicates that fire dynamics arose from changing combinations of hydroclimatic variability, vegetation, and human land use, but that their present-day convergence has generated conditions outside the range observed through most of the late Holocene.

https://doi.org/10.5194/egusphere-2026-6376
Preprint. Discussion started: 23 November 2026
© Author(s) 2026. CC BY 4.0 License.

Appendix A

A1 Stratigraphic and chronological framework

According to the stratigraphic framework established by Frugone-Álvarez et al. (2017), three major lithostratigraphic units characterize the sequence. Unit 3 (ca. 1072–578 cm; c. 6.2–2.2 cal ka BP) is dominated by finely laminated, organic-rich muds (Facies B4) intercalated with calcareous silts (Facies M2) and erosive, graded turbidites (Facies B3), recording an open coastal lagoon with elevated bioproductivity (BioSi ~ 7.9%, TOC ~ 3.5%) and persistent gypsum and calcite following the mid-Holocene marine transgression. Unit 2 (578–284 cm; c. 2.2–1.0 cal ka BP) represents a restricted bay subdivided into Subunit 2B (578–380 cm), which preserves the highest values of the sequence for TOC (4.2%), BioSi (7.1%), and authigenic pyrite under persistent bottom-water anoxia and Subunit 2A (380–284 cm), where banded-to-laminated muds (Facies B1) capture a sharp decline in BioSi, Ca, and Sr during a brackish-to-freshwater transition. Unit 1 (284–0 cm; last c. 1.0 cal ka BP) marks the definitive closure to the ocean, comprising Subunit 1C (284–170 cm) with baseline organic-poor lacustrine muds (Facies L3) devoid of carbonates; Subunit 1B (169–64 cm), defined by prominent increases in magnetic susceptibility, XARM, detrital quartz, and chlorite; and Subunit 1A (63–0 cm), characterized by alternating black and brown muds (Facies L1–L2) and exotic *Pinus* pollen reflecting accelerated watershed erosion and historical anthropogenic destabilization.

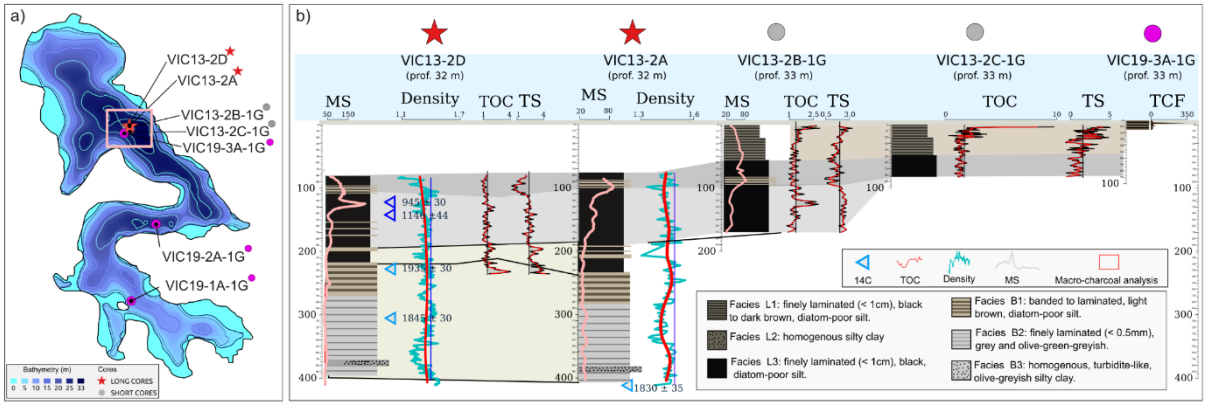

Fig. A1. Composite sedimentary sequence and coring locations at Lake Vichuquén.

a) Bathymetric map showing the distribution of long (red stars) and short (grey and purple circles) sediment cores. The red box highlights the primary coring area from which the composite sequence was extracted for macro-charcoal analysis. b) Lithostratigraphic correlation framework for the studied cores. Correlation is based on sedimentary facies, magnetic susceptibility (MS), dry bulk density, total organic carbon (TOC), and total sulfur (TS) records (Frugone-Álvarez et al., 2017). Blue triangles indicate radiocarbon (^{14}C) tie points. The total charcoal frequency (TCF) profile for the short core VIC19-3A-1G is shown on the far right.

https://doi.org/10.5194/egusphere-2026-6376
Preprint. Discussion started: 23 November 2026
© Author(s) 2026. CC BY 4.0 License.

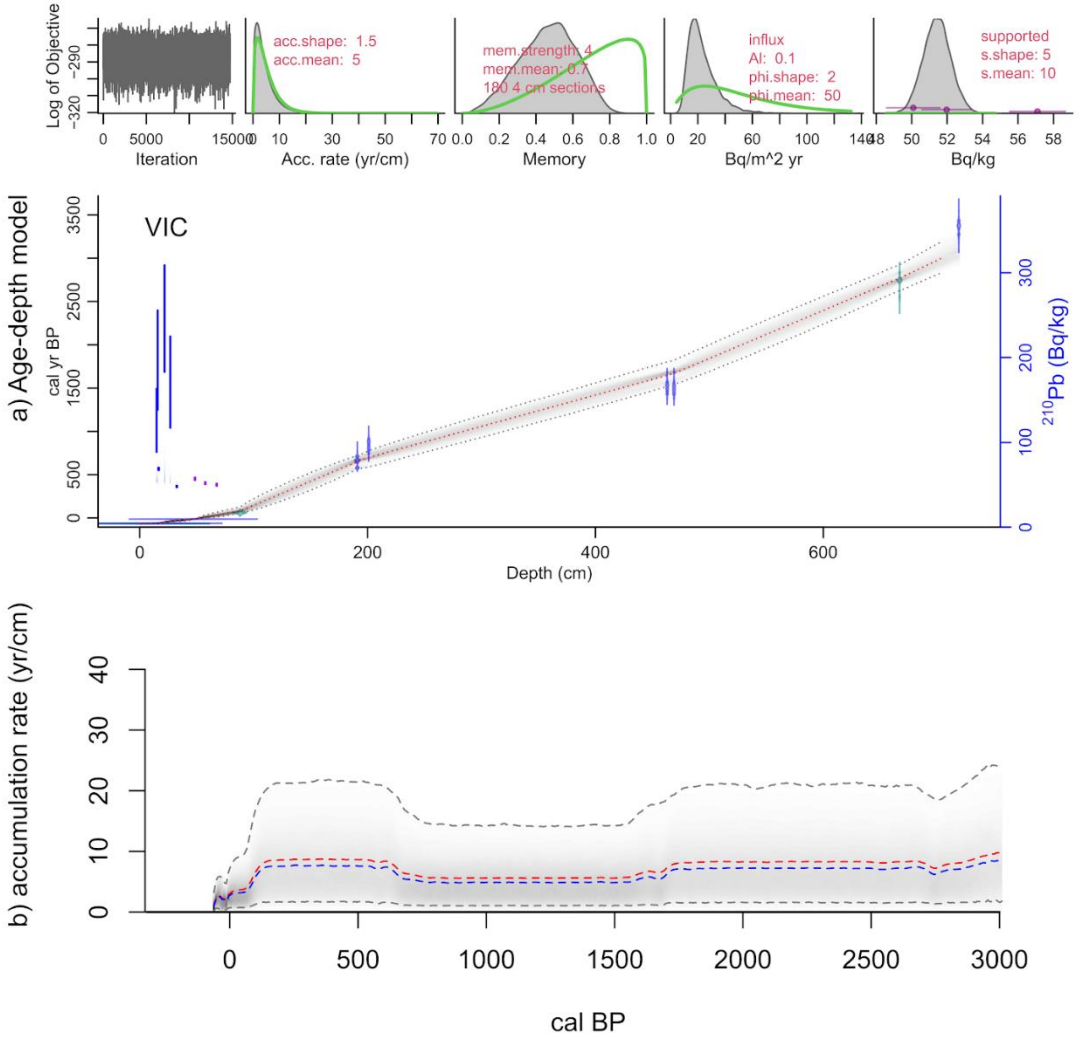

Fig. A2. Bayesian age-depth model and accumulation rates for the VIC sequence integrating ^{210}Pb and ^{14}C data (*rplum* v1.0.0). (a) Age-depth trajectory displaying the modeled mean age (red dotted line) and 95% confidence intervals (grey envelope), with a mean error range of 230.7 yr (spanning 0.9 yr at 1 cm to 355.2 yr at 704 cm). ^{14}C dates and ^{210}Pb distributions are shown in blue. Posterior parameter estimates include mean accumulation rate (4.38 yr/cm), memory (0.47), ^{210}Pb influx (35.13), and supported ^{210}Pb (50.36). (b) Estimated sediment accumulation rate (yr/cm) over time (cal yr BP), showing the mean rate (red dashed line) and 95% confidence intervals (grey envelope).

A2 Spectral analysis via REDFIT

Spectral analysis is a powerful statistical method to estimate and study the spectrum for any stationary time series. However, the great number of these methods require that the time series under analysis are evenly spaced in time (regular time series)

https://doi.org/10.5194/egusphere-2026-6376
Preprint. Discussion started: 23 November 2026
© Author(s) 2026. CC BY 4.0 License.

and paleoclimate time series are not generally evenly spaced. One way to address this drawback is to "transform" the unevenly spaced time series to regular data through interpolation methods and after that apply any standard spectral analysis method, but interpolation might alter the estimation of the spectrum and introduce bias (Schulz and Statteger 1997; Schulz and Mudelsee 2002, Polanco-Martínez and Faria 2018, among others). Schulz and Mudelsee (2002) developed a statistical-computational method to estimate the spectrum directly (interpolation is not required) for unevenly spaced paleoclimate time series via the Lomb-Scargle Fourier transform (LSFT) (Lomb 1976; Scargle 1982), which is widely used in the paleoclimate community. REDFIT takes into account the red-noise signature of the climate system (see, e.g. Gilman et al. 1963 or Hasselmann 1976, among others) fitting an AR1 (autoregressive process of order 1) model. REDFIT also includes the Welch-overlapped-segment-averaging (WOSA) procedure (Welch, 1967) to smooth the spectrum to obtain a consistent (in statistical sense) one. REDFIT uses a parametric approach, i.e. the theoretical AR1 spectrum (chi^2) to obtain statistical significance and other nonparametric method through Monte-Carlo simulations; the confidence levels estimated by REDFIT are 80, 90, 95 and 99%, and we included the 90, 95 and 99% in our analysis. We removed the linear trend in all paleoclimate data under study before estimating the spectrum to satisfy the stationary property and used the following parameters to estimate the smoothed spectrum (with 8 degrees of freedom): n50=6 (Welch window's number. We used some different values and results did not change substantially), iwin=0 (rectangular, but other kinds of windows were used and results do not change substantially) and NSim (Monte Carlo simulations)=5000. We utilized the original Fortran 90 program (Ver. 3.8) (Schulz and Mudelsee 2002).

https://doi.org/10.5194/egusphere-2026-6376
Preprint. Discussion started: 23 November 2026
© Author(s) 2026. CC BY 4.0 License.

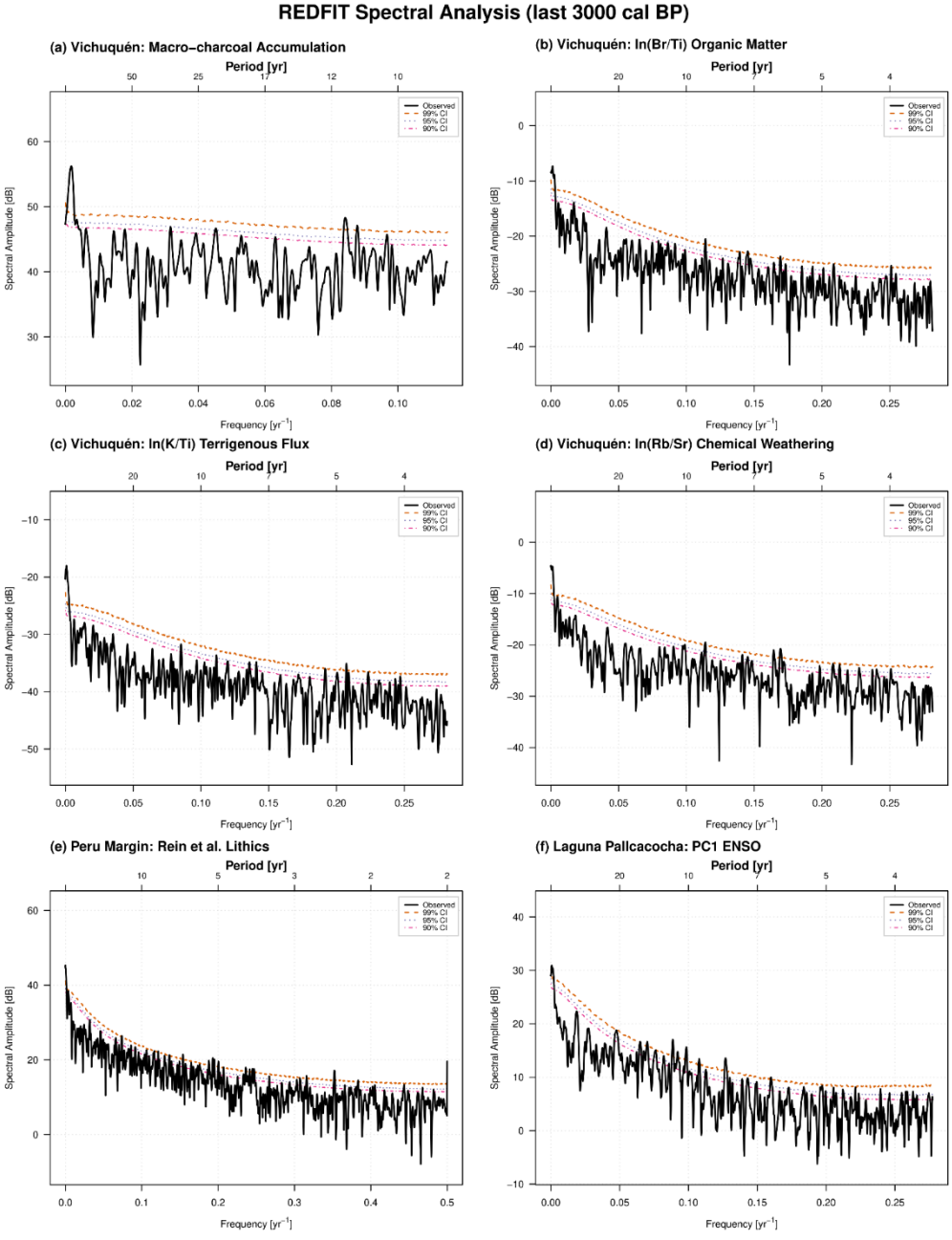

Fig. A3. REDFIT red-noise spectral analysis of paleoenvironmental proxies and regional teleconnection records for the last 3,000 cal yr BP. (a) Lake Vichuquén macro-charcoal accumulation rate. (b) Lake Vichuquén ln(Br/Ti) ratio. (c) Lake Vichuquén ln(K/Ti) ratio (d) Lake Vichuquén ln(Rb/Sr) ratio. (e) Lithic flux from Rein et al. 2005 (coastal El Niño). (f) Laguna Pallcacocha PC1 score from Moy et al., 2002 (tropical Pacific ENSO-band variability). In all panels, the solid black curves represent the sample spectrum expressed in decibels (dB). Theoretical first-order autoregressive AR(1) red-

https://doi.org/10.5194/egusphere-2026-6376
Preprint. Discussion started: 23 November 2026
© Author(s) 2026. CC BY 4.0 License.

noise background false-alarm significance levels generated via 5,000 parametric Monte Carlo simulations are indicated by dashed brown (90%), purple (95%), and red (99%) curves. The bottom axes indicate frequencies (yr^{-1}) and the top axes denote harmonic periods (yr).

A3 Wavelet spectral analysis via the WWZ

In addition to REDFIT, we have also used a novel statistical-computational tool to estimate the wavelet spectrum (uni- and bi-variate cases) for unevenly spaced (interpolation is not required) time series that was recently implemented in the Python package Pyleoclim (Khider et al. 2022). This method is based on the Weighted wavelet Z-transform (WWZ) (Foster 1996) and includes some improvements proposed by Kirchner & Neal (2013). The WWZ is based on the Morlet wavelet function and uses least-squares minimization to suppress the energy leakage caused by the data gaps (Foster 1996, Khider et al. 2022). The key adjustable parameter in the estimation of the WWZ is the decay constant c. This is used to produce a balance between time and scale (frequency) resolutions and we utilized the value 1/(8pi^2) such as was suggested in several authors (e.g. Witt and Schumann 2005, Polanco-Martínez and Faria 2018, among others). One advantage of the wavelet spectral analysis is that it is able to tackle both stationary and non-stationary time series (many paleoclimate time series fall into this category). The WWZ in paleoclimate was introduced by Witt and Schumann in 2005, but the computational implementation was not available and perhaps for this reason this method has not been extensively used in paleoclimate. Pyleoclim includes the estimation of spectrum for the uni- and bi-variate cases (wavelet coherence), and we have used this last tool to study the relationships between the time series analysed. Pyleoclim also uses an AR1 model and Monte-Carlo simulations to estimate the statistical significance, which is done for several levels of confidence although we use the 95% level.

A4 References

Foster, G.: Wavelets for period analysis of unevenly sampled time series, The Astronomical Journal, 112, 1709–1729, 1996.

Gilman, D. L., Fuglister, F. J., and Mitchell Jr, J. M.: On the power spectrum of “red noise,” Journal of Atmospheric Sciences, 20, 182–184, 1963.

Hasselmann, K.: Stochastic climate models: Part I. Theory, Tellus A: Dynamic Meteorology and Oceanography, 28, 473, https://doi.org/10.3402/tellusa.v28i6.11316, 1976.

Khider, D., Emile-Geay, J., Zhu, F., James, A., Landers, J., Ratnakar, V., and Gil, Y.: Pyleoclim: Paleoclimate Timeseries Analysis and Visualization With Python, Paleoceanog and Paleoclimatol, 37, e2022PA004509, https://doi.org/10.1029/2022PA004509, 2022.

Kirchner, J. W. and Neal, C.: Universal fractal scaling in stream chemistry and its implications for solute transport and water quality trend detection, Proc. Natl. Acad. Sci. U.S.A., 110, 12213–12218, https://doi.org/10.1073/pnas.1304328110, 2013.

Lomb, N. R.: Least-squares frequency analysis of unequally spaced data, Astrophys Space Sci, 39, 447–462, https://doi.org/10.1007/BF00648343, 1976.

https://doi.org/10.5194/egusphere-2026-6376
Preprint. Discussion started: 23 November 2026
© Author(s) 2026. CC BY 4.0 License.



Polanco-Martínez, J. M. and Faria, S. H.: Estimation of the significance of the Foster's wavelet spectrum by means of the permutation test, and applications to paleoclimate records, Boletin Geologico Y Minero, 129, 2018.

Scargle, J. D.: Studies in astronomical time series analysis. II-Statistical aspects of spectral analysis of unevenly spaced data, Astrophysical Journal, Part 1, vol. 263, Dec. 15, 1982, p. 835-853., 263, 835–853, 1982.

Schulz, M. and Mudelsee, M.: REDFIT: estimating red-noise spectra directly from unevenly spaced paleoclimatic time series, Computers & Geosciences, 28, 421–426, 2002.

Schulz, M. and Stattegger, K.: SPECTRUM: Spectral analysis of unevenly spaced paleoclimatic time series, Computers & Geosciences, 23, 929–945, 1997.

Welch, P.: The use of fast Fourier transform for the estimation of power spectra: A method based on time averaging over short, modified periodograms, IEEE Transactions on audio and electroacoustics, 15, 70–73, 1967.

Witt, A. and Schumann, A. Y.: Holocene climate variability on millennial scales recorded in Greenland ice cores, Nonlinear Processes in Geophysics, 12, 345–352, 2005.

https://doi.org/10.5194/egusphere-2026-6376
Preprint. Discussion started: 23 November 2026
© Author(s) 2026. CC BY 4.0 License.

834 **Appendix B: Additional proxy data and analyses**

835

836

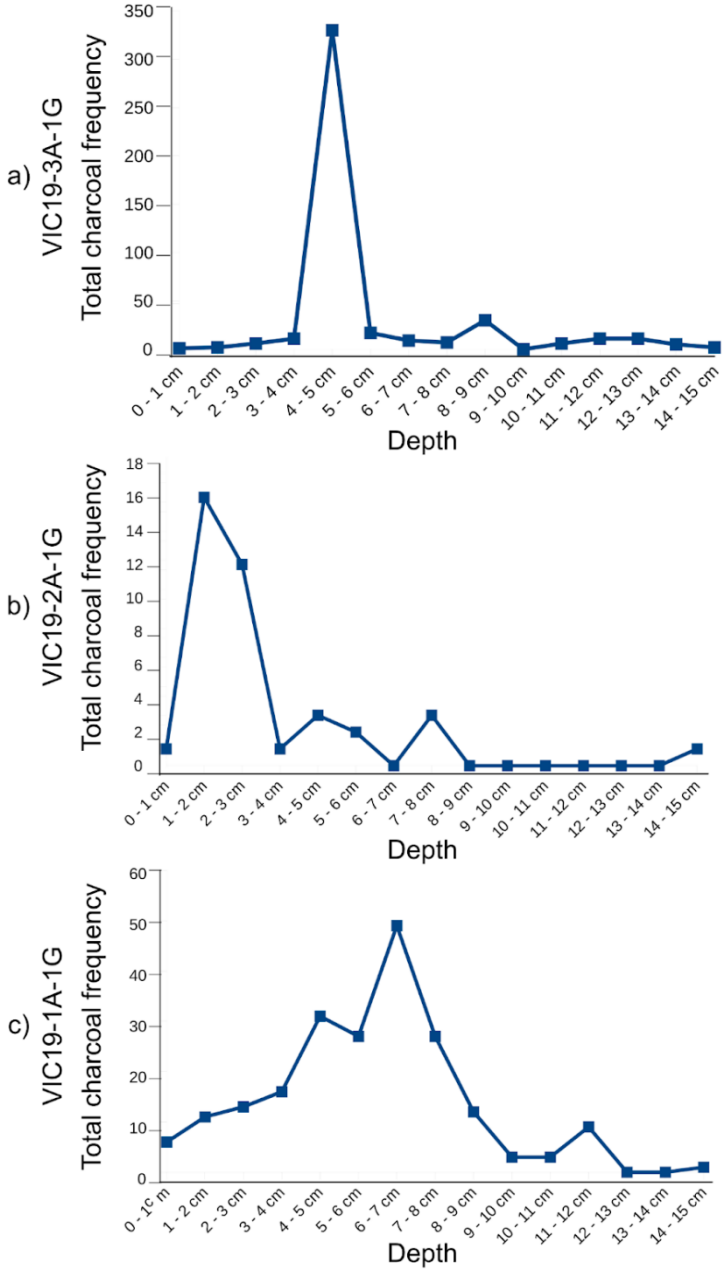

837

838 **Fig. B1.** Total charcoal frequency from VIC19-3A-1G, VIC19-2A-1G, VIC19-1A-1G cores.

https://doi.org/10.5194/egusphere-2026-6376
Preprint. Discussion started: 23 November 2026
© Author(s) 2026. CC BY 4.0 License.

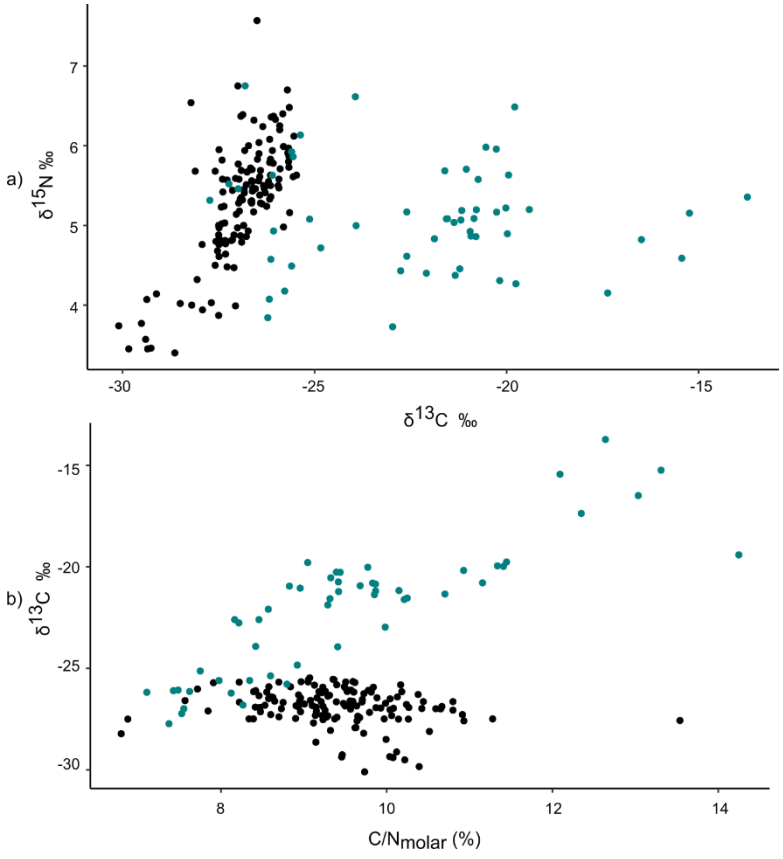

Fig. B2. Summary of the distribution of isotopic data from the sediments of the Lake Vichuquén in the complete composite sequence (VIC19-3A-1G, VIC13-2B-1G, VIC13-2D and VIC13-2A). a) $\delta^{13}C$ and $\delta^{15}N$ values b) $\delta^{13}C$ and C/Nmolar values. Black points data from Fuentealba et al., 2021 (samples of c. last 500 years), Cyan points data from this study (samples of c. 500 - 3000 cal yrs BP).

https://doi.org/10.5194/egusphere-2026-6376
Preprint. Discussion started: 23 November 2026
© Author(s) 2026. CC BY 4.0 License.

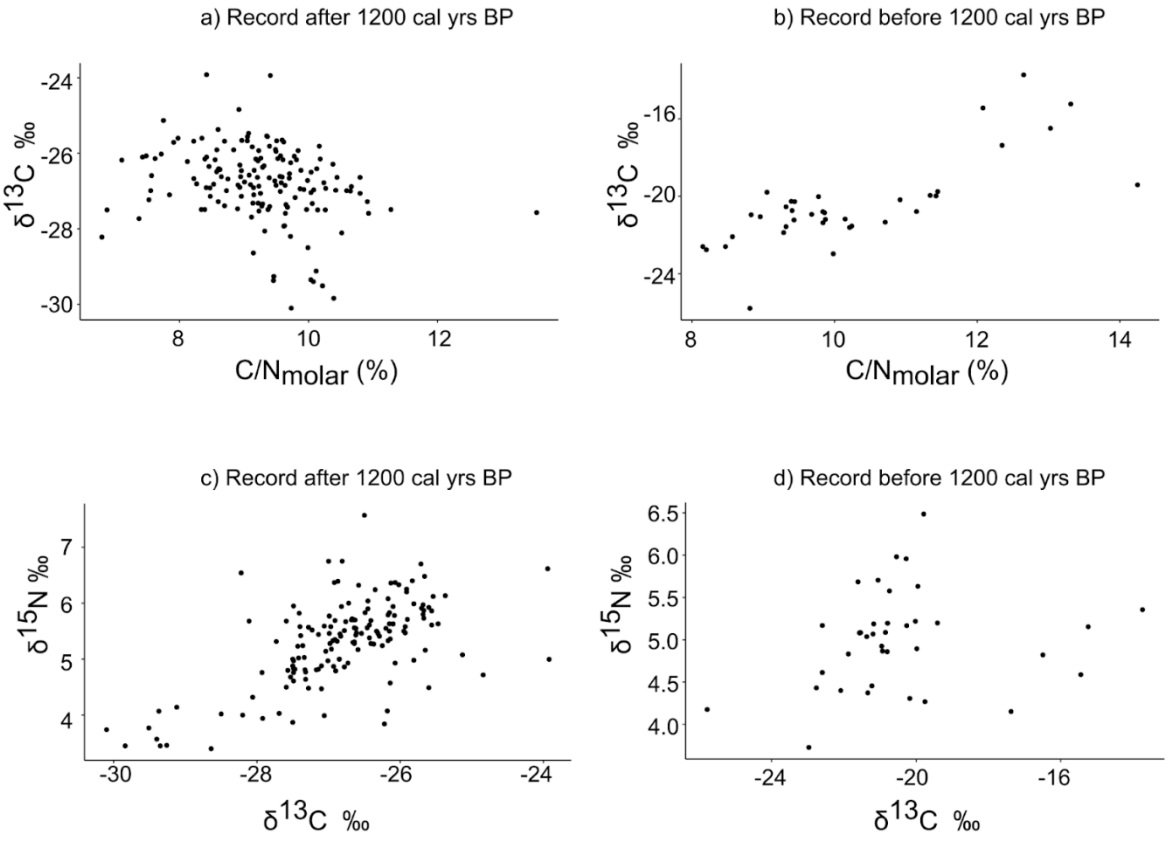

Fig. B3. Summary of the distribution of isotopic data before and after 1,200 cal yr BP, from the sediments of the Lake Vichuquén composite sequence (VIC19-3A-1G, VIC13-2B-1G, VIC13-2D and VIC13-2A). a) $\delta^{13}C$ and C/Nmolar values after 1,200 cal yr BP. b) $\delta^{13}C$ and C/Nmolar values before 1,200 cal yr BP. c) $\delta^{15}N$ and $\delta^{13}C$ values after 1,200 cal yr BP. d) $\delta^{15}N$ and $\delta^{13}C$ values before 1,200 cal yr BP.

https://doi.org/10.5194/egusphere-2026-6376
Preprint. Discussion started: 23 November 2026
© Author(s) 2026. CC BY 4.0 License.

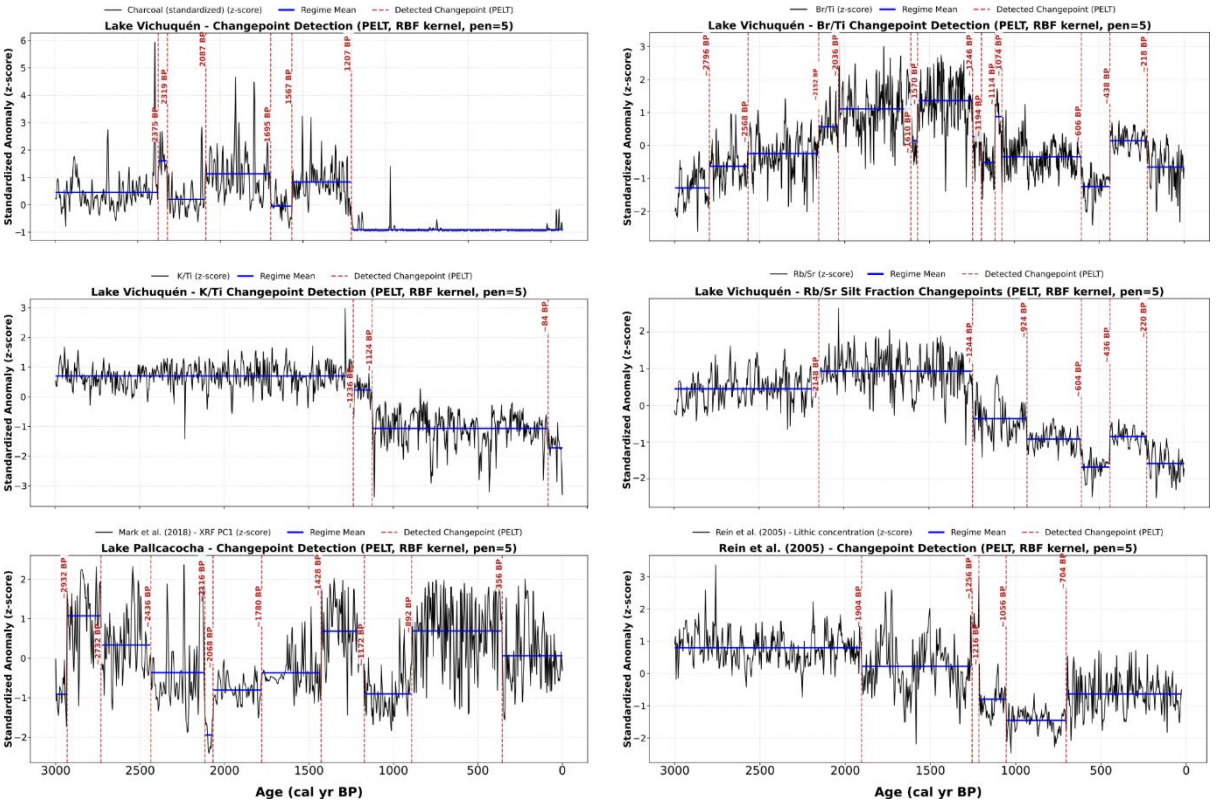

Fig. B4. Changepoint analysis across Late Holocene sedimentary records (0–3000 cal yr BP). Statistical regimes identified via the PELT algorithm (RBF kernel, pen = 5, minimum segment size = 40 yr) applied to standardized anomalies (z-scores). Black curves denote normalized time series, solid blue lines mark mean values for each regime, and red dashed vertical lines indicate detected changepoints labeled with transition ages in cal yr BP. (a) Standardized sedimentary charcoal (CHAR) record from Lake Vichuquén (paleofires). (b) Lake Vichuquén Br/Ti ratio (lacustrine bioproductivity). (c) Lake Vichuquén K/Ti ratio (detrital transport). (d) Lake Vichuquén Rb/Sr ratio (water balance). (e) Lake Pallcacocha XRF PC1 (regional hydroclimate/ENSO; Mark et al., 2018). (f) Marine coastal lithics from Peru (ENSO-driven flood events; Rein et al., 2005). Horizontal time axes are reversed, with the present to the right.

https://doi.org/10.5194/egusphere-2026-6376
Preprint. Discussion started: 23 November 2026
© Author(s) 2026. CC BY 4.0 License.

Sample	Depth (cm)	Level cal yr BP (Median)	Wavy top rondels	Discriminant function of cross-shaped phytoliths
VIC1	165	503	Presence	positive maize prediction (0.69)
VIC2	195	671	Presence	
VIC3	226	788		positive maize prediction (0.75)
VIC5	284	966	Presence	positive maize prediction (0.7)
VIC7	343	1210		positive maize prediction (0.69)
VIC8	480	1740		positive maize prediction (0.67)
VIC9	510	1895	Presence	
VIC10	542	2067		positive maize prediction (0.6)

Table B1. Summary of the samples from the compiled Vichuquén Lake sediment core with the presence of wavy top rondels and / or positive phytoliths for the prediction of maize according to the discriminant function of cross-shaped phytoliths.

Code and data availability

The raw and processed data and analytical code supporting this study are deposited in a Zenodo research compendium. The compendium is restricted during peer review and is available to reviewers through a confidential access link provided in the submission system (cover letter). Upon acceptance, the compendium will be made publicly available, with data and documentation licensed under CC BY 4.0 and code under the MIT License. Third-party datasets are cited in the manuscript and their sources are documented in the compendium.

Author contributions

CGA was responsible for conceptualization, methodology, investigation, formal analysis, project administration, funding acquisition, and writing – original draft preparation. MFA contributed to conceptualization, investigation, formal analysis, data curation, visualization, funding acquisition, and writing – review and editing. MF contributed to investigation, formal analysis (stable isotopes), and writing – review and editing. JMPM was responsible for formal analysis (statistical analyses) and contributed to methodology. AM contributed to investigation, formal analysis (pollen), and writing – review and editing. MG contributed to investigation, formal analysis (stable isotopes), and writing – review and editing. RC contributed to investigation, data curation, and writing – review and editing. JI contributed to methodology, formal analysis (phytoliths), supervision, and writing – review and editing. BVG contributed to investigation, methodology, supervision, funding

https://doi.org/10.5194/egusphere-2026-6376
Preprint. Discussion started: 23 November 2026
© Author(s) 2026. CC BY 4.0 License.

acquisition, and writing – review and editing. CL contributed to conceptualization, methodology, investigation, formal analysis, supervision, project administration, funding acquisition, and writing – review and editing.

Competing interests

The authors have the following competing interests: At least one of the (co-)authors is a member of the editorial board of Climate of the Past.

Acknowledgements

We thank Graciela Gil, Penélope González, Elena Royo, Raquel López, Ignacio Jara, Leonardo Villacís, Juana Alejandra Martel, Eugenia Gayo, Mauricio Lima, Aurora Gaxiola and Karla Ojeda for their technical support with softwares, sampling and and preliminary revisions of this text. We also thank the archaeologists of the Museo de Historia Natural de Chile: Rubén Stehberg and Cristian Becker for providing us with access to unpublished reports of archaeological sites excavated around Lago Vichuquén.

Financial support

We acknowledge funding by Agencia Nacional de Investigación y Desarrollo de Chile (ANID) Fondecyt Regular 1260475, Fondecyt Regular 1241705, ANID PIA BASAL FB210006 to the IEB, from ANID FONDECYT 1231820, Millennium Science Initiative Program Nucleus AFOREST–NCS2022_24 and Universidad de Tarapaca UTA 8799−23, S/CV (2024000429). Additional support was provided by Avanza UC (ID AV25013) from Pontifical Catholic University of Chile to CL and MF.

Review statement

References

Abarzúa, A. M., Vargas, C., Jarpa, L., Gutiérrez, N. M., Hinojosa, L. F., and Paula, S.: Evidence of Neogene wildfires in central Chile: Charcoal records from the Navidad Formation, Palaeogeography, Palaeoclimatology, Palaeoecology, 459, 76–85, https://doi.org/10.1016/j.palaeo.2016.06.036, 2016.

Aldunate, C., Gallardo, F., Fernández, C., Román, A., and Deza, A.: Arqueología de la desembocadura del río Maule, in: Actas del XI Congreso Nacional de Arqueología Chilena, vol. III, Museo Nacional de Historia Natural / Sociedad Chilena de Arqueología, Santiago, 145–152, 1991.

https://doi.org/10.5194/egusphere-2026-6376
Preprint. Discussion started: 23 November 2026
© Author(s) 2026. CC BY 4.0 License.

Aleman, J. C., Canal-Subitani, S., Favier, C., and Bremond, L.: Influence of the local environment on lacustrine sedimentary phytolith records, Palaeogeography, Palaeoclimatology, Palaeoecology, 414, 273–283, https://doi.org/10.1016/j.palaeo.2014.08.030, 2014.

Aquino-López, M. A., Blaauw, M., Christen, J. A., and Sanderson, N. K.: Bayesian Analysis of ^{210} 210 Pb Dating, JABES, 23, 317–333, https://doi.org/10.1007/s13253-018-0328-7, 2018.

Armesto, J., Bustamante, M. S, and Díaz, M: Fire Disturbance Regimes, Ecosystem Recovery and Restoration Strategies in Mediterranean and Temperate Regions of Chile, in: Fire Effects on Soils and Restoration Strategies, CRC Press, Boca Raton, https://doi.org/10.1201/9781439843338, 2009.

Armesto, J. J., Manuschevich, D., Mora, A., Smith-Ramirez, C., Rozzi, R., Abarzúa, A. M., and Marquet, P. A.: From the Holocene to the Anthropocene: A historical framework for land cover change in southwestern South America in the past 15,000 years, Land Use Policy, 27, 148–160, https://doi.org/10.1016/j.landusepol.2009.07.006, 2010.

Armesto, Juan, Arroyo, M. T. K., and Hinojosa, L. F.: The Mediterranean Environment of Central Chile, in: The Physical Geography of South America, Oxford University Press, 184–199, 2007.

Armstrong, C. G., Shoemaker, A. C., McKechnie, I., Ekblom, A., Szabó, P., Lane, P. J., McAlvay, A. C., Boles, O. J., Walshaw, S., Petek, N., Gibbons, K. S., Quintana Morales, E., Anderson, E. N., Ibragimow, A., Podruczny, G., Vamosi, J. C., Marks-Block, T., LeCompte, J. K., Awâsis, S., Nabess, C., Sinclair, P., and Crumley, C. L.: Anthropological contributions to historical ecology: 50 questions, infinite prospects, PLoS ONE, 12, e0171883, https://doi.org/10.1371/journal.pone.0171883, 2017.

Bai, J. and Perron, P.: Computation and analysis of multiple structural change models, J of Applied Econometrics, 18, 1–22, https://doi.org/10.1002/jae.659, 2003.

Balée, W.: The Research Program of Historical Ecology, Annu. Rev. Anthropol., 35, 75–98, https://doi.org/10.1146/annurev.anthro.35.081705.123231, 2006.

Barichivich, J. E.: Fire in Mediterranean Climate Ecosystems—A Comparative Overview, Israel Journal of Ecology & Evolution, 58, 123–135, 2012.

Blaauw, M. and Christen, J. A.: Flexible paleoclimate age-depth models using an autoregressive gamma process, Bayesian Anal., 6, https://doi.org/10.1214/11-BA618, 2011.

Bonk, A., Kinder, M., Enters, D., Grosjean, M., Meyer-Jacob, C., and Tylmann, W.: Sedimentological and geochemical responses of Lake Żabińskie (north-eastern Poland) to erosion changes during the last millennium, J Paleolimnol, 56, 239–252, https://doi.org/10.1007/s10933-016-9910-6, 2016.

Bowman, D. M. J. S., Balch, J., Artaxo, P., Bond, W. J., Cochrane, M. A., D'Antonio, C. M., DeFries, R., Johnston, F. H., Keeley, J. E., Krawchuk, M. A., Kull, C. A., Mack, M., Moritz, M. A., Pyne, S., Roos, C. I., Scott, A. C., Sodhi, N. S., and Swetnam, T. W.: The human dimension of fire regimes on Earth: The human dimension of fire regimes on Earth, Journal of Biogeography, 38, 2223–2236, https://doi.org/10.1111/j.1365-2699.2011.02595.x, 2011.

https://doi.org/10.5194/egusphere-2026-6376
Preprint. Discussion started: 23 November 2026
© Author(s) 2026. CC BY 4.0 License.

Bullock, Dillman S: The Agricultural Conditions and Needs of the Araucanian Indians, Master's Thesis, Michigan Agricultural College, East Lansing, Michigan, USA, 1911.

Calo, David Benjamin: Sedimentary Analysis of Fire History and Paleohydrology, Eagle Lake, California 9, Master's Thesis, California State University, 2014.

Carrasco-Escaff, T., Garreaud, R., Bozkurt, D., Jacques-Coper, M., and Pauchard, A.: The key role of extreme weather and climate change in the occurrence of exceptional fire seasons in south-central Chile, Weather and Climate Extremes, 45, 100716, https://doi.org/10.1016/j.wace.2024.100716, 2024.

Chen, J., An, Z., and Head, J.: Variation of Rb/Sr Ratios in the Loess-Paleosol Sequences of Central China during the Last 130,000 Years and Their Implications for Monsoon Paleoclimatology, Quat. res., 51, 215–219, https://doi.org/10.1006/qres.1999.2038, 1999.

Cordero, R. R., Feron, S., Damiani, A., Carrasco, J., Karas, C., Wang, C., Kraamwinkel, C. T., and Beaulieu, A.: Extreme fire weather in Chile driven by climate change and El Niño–Southern Oscillation (ENSO), Sci Rep, 14, 1974, https://doi.org/10.1038/s41598-024-52481-x, 2024.

Cornejo, L: Report of radiocarbon dating analyses, Exposición Museo de Vichuquén, Vichuquén, 1988.

Cornejo, Luis, Jackson, Donald, and Saavedra Villanueva, Miguel A: Cazadores-recolectores arcaicos al sur del desierto (ca. 11.000 a 300 a.C.), in: Prehistoria en Chile. Desde sus primeros habitantes hasta los Incas, Editorial Universitaria, Santiago, Chile, 285–318, 2016.

Corporación Nacional Forestal: Plan de manejo de la Reserva Nacional Laguna Torca., Santiago, Chile, https://www.conaf.cl/centro-documental/plan-de-manejo-de-la-rn-laguna-torca/, 1990.

Corporación Nacional Forestal (Chile): Análisis de la afectación y severidad de los incendios forestales ocurridos en enero y febrero de 2017 sobre los usos de suelo y los ecosistemas naturales presentes entre las regiones de Coquimbo y la Araucanía de Chile., Corporación Nacional Forestal (CONAF), http://www.conaf.cl/tormenta_de_fuego-2017/INFORME-AFECTACION-Y_SEVERIDAD-DE-INCENDIOS-ForestalES-VERANO-2017-SOBRE-ECOSISTEMAS-VEGETACIONALES-CONAF.pdf (last access: 9 September 2026), 2017.

Correa Girrulat, Itací and Carrasco Lagos, Carolina: Tutuquén: Vestigios de los antiguos habitantes de Chile Central, Consejo de Monumentos Nacionales, Santiago, Chile, n.d.

Correa, M. C. O.: El pueblo de indios de Vichuquén: siglos XVI y XVII, Revista de Historia Indígena, Pág. 19-37, 2016.

Crema, E. R. and Bevan, A.: INFERENCE FROM LARGE SETS OF RADIOCARBON DATES: SOFTWARE AND METHODS, Radiocarbon, 63, 23–39, https://doi.org/10.1017/RDC.2020.95, 2021.

Crumley, C. L.: Historical Ecology: A Robust Bridge between Archaeology and Ecology, Sustainability, 13, 8210, https://doi.org/10.3390/su13158210, 2021.

Darin, A. V., Kalugin, I. A., Maksimov, M. A., Rogozin, D. Y., Rakshun, Ya. V., Darin, F. A., and Sorokoletov, D. S.: Reconstructing the levels of Lake Shira over the last 1500 years with an annual time scale based on data from X-Ray

https://doi.org/10.5194/egusphere-2026-6376
Preprint. Discussion started: 23 November 2026
© Author(s) 2026. CC BY 4.0 License.

fluorescence microanalysis using beams of synchrotron radiation, Bull. Russ. Acad. Sci. Phys., 79, 126–130, https://doi.org/10.3103/S1062873815010116, 2015.

Delgado, A: El registro antracológico en contextos El Vergel y Reche-Mapuche de Isla Mocha. Una aproximación a la gestión de los paisajes vegetales leñosos, Undergraduate thesis, Universidad de Chile, Santiago, Chile, 2016.

Dickau, R., Whitney, B. S., Iriarte, J., Mayle, F. E., Soto, J. D., Metcalfe, P., Street-Perrott, F. A., Loader, N. J., Ficken, K. J., and Killeen, T. J.: Differentiation of neotropical ecosystems by modern soil phytolith assemblages and its implications for palaeoenvironmental and archaeological reconstructions, Review of Palaeobotany and Palynology, 193, 15–37, https://doi.org/10.1016/j.revpalbo.2013.01.004, 2013.

Echaiz, R. L.: Prehistoria de Chile Central, Editorial Francisco de Aguirre, 166 pp., 1976.

Faegri, K., Iversen, J., Kaland, P. E., and Krzywinski, K.: Textbook of Pollen Analysis, Blackburn Press, 328 pp., 2000.

Falabella, F., Cornejo, L. E., Sanhueza, L., and Correa, I.: Trends in thermoluminescence date distributions for the Angostura micro region in Central Chile, Quaternary International, 356, 27–38, https://doi.org/10.1016/j.quaint.2014.06.049, 2015.

Falabella, F., Pavlovic, D., Planella, M. T., and Sanhueza, L.: Diversidad y heterogeneidad cultural y social en Chile Central durante los periodos Alfarero Temprano e Intermedio Tardío (300 años aC a 1.450 años dC), in: Prehistoria en Chile. Desde sus primeros habitantes hasta los Incas, Universitaria Santiago, 365–399, 2016.

Falabella, F., Sanhueza, L., Abarca, V., and Herrera, M. J.: Social differentiation in the pre-Hispanic horticultural societies of central Chile (200–1500 AD). A stable isotope study, Quaternary International, 548, 41–56, https://doi.org/10.1016/j.quaint.2019.09.021, 2020.

Frugone-Álvarez, M., Latorre, C., Giralt, S., Polanco-Martínez, J., Bernárdez, P., Oliva-Urcia, B., Maldonado, A., Carrevedo, M. L., Moreno, A., Delgado Huertas, A., Prego, R., Barreiro-Lostres, F., and Valero-Garcés, B.: A 7000-year high-resolution lake sediment record from coastal central Chile (Lago Vichuquén, 34°S): implications for past sea level and environmental variability, J Quaternary Science, 32, 830–844, https://doi.org/10.1002/jqs.2936, 2017.

Frugone-Álvarez, M., Latorre, C., Moreno, A., Maldonado, A., Santoro, C., Carrevedo, M. L., Fuentealba, M., and Valero-Garcés, B.: Cambio Global en un lago costero de Chile Central durante el último milenio, in: Cambio Global: una mirada desde Iberoamérica, Consejo Superior de Investigaciones Científicas (CSIC), 260–269, 2018.

Frugone-Álvarez, M., Latorre, C., Barreiro-Lostres, F., Giralt, S., Moreno, A., Polanco-Martínez, J., Maldonado, A., Carrevedo, M. L., Bernárdez, P., Prego, R., Delgado Huertas, A., Fuentealba, M., and Valero-Garcés, B.: Volcanism and climate change as drivers in Holocene depositional dynamic of Laguna del Maule (Andes of central Chile – 36° S), Clim. Past, 16, 1097–1125, https://doi.org/10.5194/cp-16-1097-2020, 2020.

Fuentealba, M., Latorre, C., Frugone-Álvarez, M., Sarricolea, P., Giralt, S., Contreras-Lopez, M., Prego, R., Bernárdez, P., and Valero-Garcés, B.: A combined approach to establishing the timing and magnitude of anthropogenic nutrient alteration in a mediterranean coastal lake- watershed system, Sci Rep, 10, 5864, https://doi.org/10.1038/s41598-020-62627-2, 2020.

https://doi.org/10.5194/egusphere-2026-6376
Preprint. Discussion started: 23 November 2026
© Author(s) 2026. CC BY 4.0 License.

Fuentealba, M., Latorre, C., Frugone-Álvarez, M., Sarricolea, P., Godoy-Aguirre, C., Armesto, J., Villacís, L. A., Laura Carrevedo, M., Meseguer-Ruiz, O., and Valero-Garcés, B.: Crossing a critical threshold: Accelerated and widespread land use changes drive recent carbon and nitrogen dynamics in Lake Vichuquén (35°S) in central Chile, Science of The Total Environment, 791, 148209, https://doi.org/10.1016/j.scitotenv.2021.148209, 2021.

Garreaud, R. D.: The Andes climate and weather, Adv. Geosci., 22, 3–11, https://doi.org/10.5194/adgeo-22-3-2009, 2009.

Garreaud, R. D., Alvarez-Garreton, C., Barichivich, J., Boisier, J. P., Christie, D., Galleguillos, M., LeQuesne, C., McPhee, J., and Zambrano-Bigiarini, M.: The 2010–2015 megadrought in central Chile: impacts on regional hydroclimate and vegetation, Hydrol. Earth Syst. Sci., 21, 6307–6327, https://doi.org/10.5194/hess-21-6307-2017, 2017.

Garreaud, R. D., Boisier, J. P., Rondanelli, R., Montecinos, A., Sepúlveda, H. H., and Veloso-Aguila, D.: The Central Chile Mega Drought (2010–2018): A climate dynamics perspective, Intl Journal of Climatology, 40, 421–439, https://doi.org/10.1002/joc.6219, 2020.

Gayo, E. M., McRostie, V. B., Campbell, R., Flores, C., Maldonado, A., Uribe-Rodriguez, M., Moreno, P. I., Santoro, C. M., Christie, D. A., Muñoz, A. A., and Gallardo, L.: Geohistorical records of the Anthropocene in Chile, Elementa: Science of the Anthropocene, 7, 15, https://doi.org/10.1525/elementa.353, 2019.

Giraldo Cañas, D. A., Peterson, P. M., and Sánchez Vega, I.: The genus Eragrostis (Poaceae: Chloridoideae) in northwestern South America (Colombia, Ecuador, and Peru): morphological and taxonomic studies, Universidad Nacional de Colombia. Instituto de Ciencias Naturales, 2012.

Godoy, M.: Estacionalidad y manejo de recursos naturales del bosque templado: Una aproximación etnográfica y etnoarqueológica en la cuenca fluvial Valdivia, rev.austral.cienc.soc, 73–95, https://doi.org/10.4206/rev.austral.cienc.soc.2008.n15-06, 2008.

Godoy-Aguirre, C., Frugone-Álvarez, M., Gayo, E. M., Campbell, R., Lima, M., Maldonado, A., and Latorre, C.: Population dynamics and cultural niche construction during the Late Holocene in a mediterranean ecosystem (central Chile, 32°S–36°S), The Holocene, 34, 509–518, https://doi.org/10.1177/09596836231225722, 2024.

Gómez-González, S., González, M. E., Paula, S., Díaz-Hormazábal, I., Lara, A., and Delgado-Baquerizo, M.: Temperature and agriculture are largely associated with fire activity in Central Chile across different temporal periods, Forest Ecology and Management, 433, 535–543, https://doi.org/10.1016/j.foreco.2018.11.041, 2019.

González de Nájera, A. and Donoso Rodríguez, M.: Desengaño y reparo de la Guerra del Reino de Chile, Primera edición., Universidad de los Andes. Instituto de Literatura : EU Editorial Universitaria, Santiago de Chile, 748 pp., 2017.

González, M. E., Lara, A., Urrutia, R., and Bosnich, J.: Cambio climático y su impacto potencial en la ocurrencia de incendios forestales en la zona centro-sur de Chile (33º - 42º S), Bosque (Valdivia), 32, 215–219, https://doi.org/10.4067/S0717-92002011000300002, 2011.

Guevara, Tomás: Historia de Curicó, Imprenta Victoria, Santiago de Chile, 1890.

https://doi.org/10.5194/egusphere-2026-6376
Preprint. Discussion started: 23 November 2026
© Author(s) 2026. CC BY 4.0 License.

Harris, D., Horwáth, W. R., and Van Kessel, C.: Acid fumigation of soils to remove carbonates prior to total organic carbon or CARBON-13 isotopic analysis, Soil Science Soc of Amer J, 65, 1853–1856, https://doi.org/10.2136/sssaj2001.1853, 2001.

Heusser, C. J.: Pollen and spores of Chile: modern types of the Pteridophyta, Gymnospermae, and Angiospermae, University of Arizona Press, Tucson, 167 pp., 1971.

Heusser, C. J.: Quaternary Pollen Record from Laguna de Tagua Tagua, Chile, Science, 219, 1429–1432, https://doi.org/10.1126/science.219.4591.1429, 1983.

Higuera, Philip: CharAnalysis (0.9), 2009.

Hogg, A. G., Heaton, T. J., Hua, Q., Palmer, J. G., Turney, C. S., Southon, J., Bayliss, A., Blackwell, P. G., Boswijk, G., Bronk Ramsey, C., Pearson, C., Petchey, F., Reimer, P., Reimer, R., and Wacker, L.: SHCal20 Southern Hemisphere Calibration, 0–55,000 Years cal BP, Radiocarbon, 62, 759–778, https://doi.org/10.1017/RDC.2020.59, 2020.

International Committee for Phytolith Taxonomy (ICPT), Neumann, K., Strömberg, C. A. E., Ball, T., Albert, R. M., Vrydaghs, L., and Cummings, L. S.: International Code for Phytolith Nomenclature (ICPN) 2.0, Annals of Botany, 124, 189–199, https://doi.org/10.1093/aob/mcz064, 2019.

Jenny, B., Valero-Garcés, B. L., Urrutia, R., Kelts, K., Veit, H., Appleby, P. G., and Geyh, M.: Moisture changes and fluctuations of the Westerlies in Mediterranean Central Chile during the last 2000 years: The Laguna Aculeo record (33°50′S), Quaternary International, 87, 3–18, https://doi.org/10.1016/S1040-6182(01)00058-1, 2002.

Jenny, B., Wilhelm, D., and Valero-Garcés, B.: The Southern Westerlies in Central Chile: Holocene precipitation estimates based on a water balance model for Laguna Aculeo (33°50′S), Climate Dynamics, 20, 269–280, https://doi.org/10.1007/s00382-002-0267-3, 2003.

Jin, Z., Wang, S., Shen, J., Zhang, E., Li, F., Ji, J., and Lu, X.: Chemical weathering since the Little Ice Age recorded in lake sediments: a high-resolution proxy of past climate, Earth Surf Processes Landf, 26, 775–782, https://doi.org/10.1002/esp.224, 2001.

Juggins, S.: rioja: Analysis of Quaternary Science Data (1.0-7), https://cran.r-project.org/web/packages/rioja/index.html (last access: 9 September 2026), 2024.

Kalugin, I., Selegei, V., Goldberg, E., and Seret, G.: Rhythmic fine-grained sediment deposition in Lake Teletskoye, Altai, Siberia, in relation to regional climate change, Quaternary International, 136, 5–13, https://doi.org/10.1016/j.quaint.2004.11.003, 2005.

Khider, D., Emile-Geay, J., Zhu, F., James, A., Landers, J., Ratnakar, V., and Gil, Y.: Pyleoclim: Paleoclimate Timeseries Analysis and Visualization With Python, Paleoceanog and Paleoclimatol, 37, e2022PA004509, https://doi.org/10.1029/2022PA004509, 2022.

Killick R, Eckley IA.: Changepoint: An R Package for Changepoint Analysis." Journal of Statistical Software, 58(3), 1–19. https://www.jstatsoft.org/article/view/v058i03, 2014.

https://doi.org/10.5194/egusphere-2026-6376
Preprint. Discussion started: 23 November 2026
© Author(s) 2026. CC BY 4.0 License.

Kirchner, J. W. and Neal, C.: Universal fractal scaling in stream chemistry and its implications for solute transport and water quality trend detection, Proc. Natl. Acad. Sci. U.S.A., 110, 12213–12218, https://doi.org/10.1073/pnas.1304328110, 2013.

Maas, C.: Documentación: viaje a través de las provincias australes de la República de Chile desde enero hasta junio de 1847 - Memoria Chilena, Documentos de Revista Cóndor., 1847.

Maher, L. J.: Pollen Analyses of Surface Materials from the Southern San Juan Mountains, Colorado, Geol Soc America Bull, 74, 1485, https://doi.org/10.1130/0016-7606(1963)74%255B1485:PAOSMF%255D2.0.CO;2, 1963.

Maher, L. J.: Absolute Pollen Diagram of Redrock Lake, Boulder County, Colorado, Quat. res., 2, 531–553, https://doi.org/10.1016/0033-5894(72)90090-7, 1972.

Maldonado, A. and Villagrán, C.: Paleoenvironmental Changes in the Semiarid Coast of Chile (~32°S) during the Last 6200 cal Years Inferred from a Swamp–Forest Pollen Record, Quat. res., 58, 130–138, https://doi.org/10.1006/qres.2002.2353, 2002.

Maldonado, A. and Villagrán, C.: Climate variability over the last 9900 cal yr BP from a swamp forest pollen record along the semiarid coast of Chile, Quat. res., 66, 246–258, https://doi.org/10.1016/j.yqres.2006.04.003, 2006.

Martel-Cea, A., Maldonado, A., Grosjean, M., Alvial, I., De Jong, R., Fritz, S. C., and Von Gunten, L.: Late Holocene environmental changes as recorded in the sediments of high Andean Laguna Chepical, Central Chile (32°S; 3050 m a.s.l.), Palaeogeography, Palaeoclimatology, Palaeoecology, 461, 44–54, https://doi.org/10.1016/j.palaeo.2016.08.003, 2016.

Meyers, P. A.: Applications of organic geochemistry to paleolimnological reconstructions: a summary of examples from the Laurentian Great Lakes, Organic Geochemistry, 34, 261–289, https://doi.org/10.1016/S0146-6380(02)00168-7, 2003.

Meyers, P. A. and Teranes, J. L.: Sediment Organic Matter, in: Tracking Environmental Change Using Lake Sediments, vol. 2, edited by: Last, W. M. and Smol, J. P., Kluwer Academic Publishers, Dordrecht, 239–269, https://doi.org/10.1007/0-306-47670-3_9, 2002.

Montenegro, G., Gómez, M., Díaz, F., and Ginocchio, R.: Regeneration Potential of Chilean Matorral After Fire: An Updated View, in: Fire and Climatic Change in Temperate Ecosystems of the Western Americas, vol. 160, edited by: Veblen, T. T., Baker, W. L., Montenegro, G., and Swetnam, T. W., Springer-Verlag, New York, 381–409, https://doi.org/10.1007/0-387-21710-X_14, 2003.

Moreno, P. I., Villa-Martínez, R., Cárdenas, M. L., and Sagredo, E. A.: Deglacial changes of the southern margin of the southern westerly winds revealed by terrestrial records from SW Patagonia (52°S), Quaternary Science Reviews, 41, 1–21, https://doi.org/10.1016/j.quascirev.2012.02.002, 2012.

Moy, C. M., Seltzer, G. O., Rodbell, D. T., and Anderson, D. M.: Variability of El Niño/Southern Oscillation activity at millennial timescales during the Holocene epoch, Nature, 420, 162–165, https://doi.org/10.1038/nature01194, 2002.

Muñoz, A. A. and González, M. E.: Patrones de regeneración arbórea en claros a una década de la floración y muerte masiva de *Chusquea quila* (Poaceae) en un remanente de bosque antiguo del valle central en el centro-sur de Chile, Rev. chil. hist. nat., 82, https://doi.org/10.4067/S0716-078X2009000200002, 2009.

https://doi.org/10.5194/egusphere-2026-6376
Preprint. Discussion started: 23 November 2026
© Author(s) 2026. CC BY 4.0 License.

Oksanen, J., Simpson, G. L., Blanchet, F. G., Kindt, R., Legendre, P., Minchin, P. R., O'Hara, R. B., Solymos, P., Stevens, M. H. H., Szoecs, E., Wagner, H., Barbour, M., Bedward, M., Bengtsson, H., Bolker, B., Borcard, D., Borman, T., Carvalho, G., Chirico, M., Caceres, M. D., Durand, S., Evangelista, H. B. A., FitzJohn, R., Friendly, M., Furneaux, B., Hannigan, G., Heida, I., Hill, M. O., Lahti, L., Martino, C., McGlinn, D., Ouellette, M.-H., Cunha, E. R., Smith, T., Stier, A., Braak, C. J. F. T., and Weedon, J.: vegan: Community Ecology Package (2.7-6), https://cran.r-project.org/web/packages/vegan/index.html (last access: 9 September 2026), 2026.

Pearsall, D. M.: Paleoethnobotany, 0 ed., Routledge, https://doi.org/10.4324/9781315423098, 2016.

Planella, M. T., Falabella, F., Belmar, C., and Quiroz, L.: Huertos, chacras y sementeras. Plantas cultivadas y su participación en los desarrollos culturales de Chile central, Rev. esp. antropol. am., 44, 495–522, https://doi.org/10.5209/rev_REAA.2014.v44.n2.50727, 2015.

Pliscoff, P., Folchi, M., Aliste, E., Cea, D., and Simonetti, J. A.: Chile mega-fire 2017: An analysis of social representation of forest plantation territory, Applied Geography, 119, 102226, https://doi.org/10.1016/j.apgeog.2020.102226, 2020.

Ramírez, C., Fariña, J. M., Contreras, D., Camaño, A., San Martín, C., Molina, M., Moraga, P., Vidal, O., and Pérez, Y.: La diversidad florística del humedal "Ciénagas del Name" (Región del Maule) comparada con otros humedales costeros de Chile, Gayana Bot., 71, 108–119, https://doi.org/10.4067/S0717-66432014000100011, 2014.

Rasbold, G. G., Stevaux, J. C., Parolin, M., Leli, I. T., Luz, L. D., and Brito, H. D.: Phytoliths indicate environmental changes correlated with facies analysis in a paleo island-lake, Upper Paraná River, Brazil, Journal of South American Earth Sciences, 99, 102513, https://doi.org/10.1016/j.jsames.2020.102513, 2020.

Rees, C., Seelenfreund, A., and Lemus, M.: Informe Final Proyecto Fondecyt 1930142. Estrategias de ocupación prehispánica en la costa entre el río Mataquito y Cabo Carranza (VII Región), Archivo Nacional de la Administración, Chile, Santiago de Chile, n.d.

Rees, C., Seelenfreund, A., Torres-Mura, J. C., Westfall, C., Gálvez, Ó., and Lemus, M.: Ocupación prehispánica de la desembocadura del río Maule, Boletín del Museo Regional de la Araucanía, 5, 161–172, 1993b.

Rees, C., Seelenfreund, A., and Westfall, C.: Patrones de asentamiento y explotación de recursos en la cuenca del río Maule: Epoca prehispánica, , Gaceta Arqueológica Andina5139–159, 1993a.

Reid, S., Díaz, I. A., Armesto, J. J., and Willson, M. F.: Importance of Native Bamboo for Understory Birds in Chilean Temperate Forests, The Auk, 121, 515–525, https://doi.org/10.1093/auk/121.2.515, 2004.

Rein, B., Lückge, A., Reinhardt, L., Sirocko, F., Wolf, A., and Dullo, W.: El Niño variability off Peru during the last 20,000 years, Paleoceanography, 20, 2004PA001099, https://doi.org/10.1029/2004PA001099, 2005.

Roos, C. I., Bowman, D. M. J. S., Balch, J. K., Artaxo, P., Bond, W. J., Cochrane, M., D'Antonio, C. M., DeFries, R., Mack, M., Johnston, F. H., Krawchuk, M. A., Kull, C. A., Moritz, M. A., Pyne, S., Scott, A. C., and Swetnam, T. W.: Pyrogeography, historical ecology, and the human dimensions of fire regimes, Journal of Biogeography, 41, 833–836, https://doi.org/10.1111/jbi.12285, 2014.

https://doi.org/10.5194/egusphere-2026-6376
Preprint. Discussion started: 23 November 2026
© Author(s) 2026. CC BY 4.0 License.

Rozas, V., Le Quesne, C., Rojas-Badilla, M., González, M. E., and González-Reyes, Á.: Coupled human-climate signals on the fire history of upper Cachapoal Valley, Mediterranean Andes of Chile, since 1201 CE, Global and Planetary Change, 167, 137–147, https://doi.org/10.1016/j.gloplacha.2018.05.013, 2018.

Sanhueza, L.: Niveles de integración sociopolítica, ideología e interacción en sociedades no jerárquicas: Periodo Alfarero Temprano en Chile Central, Doctoral dissertation, Universidad de Tarapacá, Chile, 2013.

Sanhueza R, L., Cornejo B, L., and Falabella G, F.: PATRONES DE ASENTAMIENTO EN EL PERÍODO ALFARERO TEMPRANO DE CHILE CENTRAL, Chungará (Arica), 39, https://doi.org/10.4067/S0717-73562007000100007, 2007.

Seelenfreund, A., Rees, C., and Torres-Mura, J.: Informe de Avance Proyecto Fondecyt 90-524/año 1991. Estudio de patrones de asentamiento y explotación de recursos naturales en la cuenca del Río Maule (VII Región): Época prehispánica, Archivo Nacional de la Administración, Chile, 1991.

Simonetti, J. and Cornejo, L.: Economic and ecological changes: the prehistory of the Andean mountains of central Chile, in: Economic Catalysts to Ecological Change, 1990.

Smith, Edmond Reuel: Los araucanos: o, Notas sobre una gira efectuada entre las tribus indígenas de Chile meridional, Imprenta Universitaria, Santiago de Chile, 1914.

Stehberg, R. and Quevedo, S.: El sitio arqueológico Paula de Vichuquén, Museo Nacional de Historia Natural, 1988.

Stehberg, R., Osorio, G., and Cerda, J. C.: Mapocho incaico central: distritos prehispánicos de irrigación, Publicación ocasional del Museo Nacional de Historia Natural, 71, 5–60, 2021.

Stockmarr, J.: Tables with spores used in absolute pollen analysis, Pollen et spores, 13, 615–621, 1971.

Torres-Ramírez, P., Ortiz, J., Figueroa, S., Jerez, R., and Arcos, D.: Characterization of the Coastal Wetland Mataquito, Curico Province, Maule Region, in: The Ecology and Natural History of Chilean Saltmarshes, edited by: Fariña, J. M. and Camaño, A., Springer International Publishing, Cham, 221–264, https://doi.org/10.1007/978-3-319-63877-5_8, 2017.

Uribe, M. and Sánchez, R.: Los incas en Chile. Aportes de la arqueología chilena a la historia del Tawantinsuyo (ca. 1.400 a 1.536 años dC), Prehistoria en Chile. Desde sus primeros habitantes hasta los Incas, 529–572, 2016.

Urrutia-Jalabert, R., González, M. E., González-Reyes, Á., Lara, A., and Garreaud, R.: Climate variability and forest fires in central and south-central Chile, Ecosphere, 9, e02171, https://doi.org/10.1002/ecs2.2171, 2018.

Villagrán, C. and Varela, J.: Palynological Evidence for Increased Aridity on the Central Chilean Coast during the Holocene, Quat. res., 34, 198–207, https://doi.org/10.1016/0033-5894(90)90031-F, 1990.

Villa-Martinez, R. and Villagrán, C.: Historia de la vegetación de bosques pantanosos de la costa de Chile central durante el Holoceno medio y tardío, Revista chilena de historia natural, 70, 391–401, 1997.

Villa-Martínez, R., Villagrán, C., and Jenny, B.: The last 7500 cal yr B.P. of westerly rainfall in Central Chile inferred from a high-resolution pollen record from Laguna Aculeo (34°S), Quat. res., 60, 284–293, https://doi.org/10.1016/j.yqres.2003.07.007, 2003.

Villa-Martínez, R., Villagrán, C., and Jenny, B.: Pollen evidence for late-Holocene climatic variability at Laguna de Aculeo, Central Chile (lat. 34°S), The Holocene, 14, 361–367, https://doi.org/10.1191/0959683604hl712rp, 2004.

https://doi.org/10.5194/egusphere-2026-6376
Preprint. Discussion started: 23 November 2026
© Author(s) 2026. CC BY 4.0 License.

Villa-Martínez, Rodrigo: Historia del clima y la vegetación de Chile central durante el Holoceno: una reconstrucción basada en el análisis de polen, sedimentos, microalgas y carbón, Doctoral dissertation, Universidad de Chile, Santiago, Chile, 2002.

Vivar, J. de: Crónica de los reinos de Chile, Historia 16, 376 pp., 1988.

Von Gunten, L., Grosjean, M., Rein, B., Urrutia, R., and Appleby, P.: A quantitative high-resolution summer temperature reconstruction based on sedimentary pigments from Laguna Aculeo, central Chile, back to AD 850, The Holocene, 19, 873–881, https://doi.org/10.1177/0959683609336573, 2009.

Whitlock, C. and Anderson, R. S.: Fire History Reconstructions Based on Sediment Records from Lakes and Wetlands, in: Fire and Climatic Change in Temperate Ecosystems of the Western Americas, vol. 160, edited by: Veblen, T. T., Baker, W. L., Montenegro, G., and Swetnam, T. W., Springer-Verlag, New York, 3–31, https://doi.org/10.1007/0-387-21710-X_1, 2003.

Whitlock, C. and Larsen, C.: Charcoal as a Fire Proxy, in: Tracking Environmental Change Using Lake Sediments, vol. 3, edited by: Smol, J. P., Birks, H. J. B., Last, W. M., Bradley, R. S., and Alverson, K., Springer Netherlands, Dordrecht, 75–97, https://doi.org/10.1007/0-306-47668-1_5, 2002.

Whitlock, C., Bianchi, M. M., Bartlein, P. J., Markgraf, V., Marlon, J., Walsh, M., and McCoy, N.: Postglacial vegetation, climate, and fire history along the east side of the Andes (lat 41–42.5°S), Argentina, Quat. res., 66, 187–201, https://doi.org/10.1016/j.yqres.2006.04.004, 2006.

Whitlock, C., Higuera, P. E., McWethy, D. B., and Briles, C. E.: Paleoecological Perspectives on Fire Ecology: Revisiting the Fire-Regime Concept~!2009-09-02~!2009-11-09~!2010-03-05~!, TOECOLJ, 3, 6–23, https://doi.org/10.2174/1874213001003020006, 2010.

Wickham, H., Chang, W., Henry, L., Pedersen, T. L., Takahashi, K., Wilke, C., Woo, K., Yutani, H., Dunnington, D., Brand, T. van den, Posit, and PBC: ggplot2: Create Elegant Data Visualisations Using the Grammar of Graphics (4.0.3), https://cran.r-project.org/web/packages/ggplot2/index.html (last access: 9 September 2026), 2026.

Winckler Grez, P., Aguirre, C., Farías, L., Contreras-López, M., and Masotti, Í.: Evidence of climate-driven changes on atmospheric, hydrological, and oceanographic variables along the Chilean coastal zone, Climatic Change, 163, 633–652, https://doi.org/10.1007/s10584-020-02805-3, 2020.